RESEARCH ARTICLE

Nanocellulose-based Hydrogels: Preparation Strategies, Dye Adsorption and Factors Impacting

Article history:
Received: 12-06-2023
Revised: 11-10-2023
Accepted: 15-10-2023

Ashvinder K. Rana[a]

Abstract: The improper disposal of dyes without any prior treatment is one of the main causes of water pollution around the globe. Since dye-contaminated water contains a variety of hazardous elements, which may harm the aquatic ecosystem, impact the aquatic organisms and ultimately enter the food web chain. The most effective ways to recycle dye-contaminated waste water are adsorption, electrolysis, advanced oxidation, etc. Out of these techniques, adsorption strategy, due to its superior physico-chemical features, has been preferably employed for treating polluted water. In this review article, the potential of pure nitrocellulose (NC) hydrogel, metal/metal oxide or photo-adsorbents-based, metal-organic-framework supported, surface functionalized, bio-materials filled NC-based hydrogels for dyes adsorption has been thoroughly reviewed. The impact of different factors such as pH, time, temperature and filler/additives on dye adsorption/degradation capability of NC-based adsorbents, and kinetic and isotherm data of dye adsorption has been assessed systematically. Further, the influence of different eluents on the recycling ability of various NC- based hydrogels has also been fully assessed.

Keywords: Nanocellulose; hydrogels; dye adsorption; kinetics study; recycle; chemical cross-linking.

1. INTRODUCTION

Supplying fresh and drinkable water is one of the biggest challenges throughout the world. In recent years, there has been a continuous rise in the pollution of natural resources, a problem which has to be addressed on an immediate basis to ensure the survival of living beings (Kaushik *et al.*, 2022; Paul & Ahankari, 2023; Solayman *et al.*, 2023). Any change in chemical, physical and biological properties of water because of aggress or access to toxic chemicals is considered as water pollution. Illegal discharge of contaminated water is a global challenge and is of great environmental concern, as fresh water resources are degrading rapidly. The current worldwide water usage is about forty-six hundred km^3/year, and according to Burek *et al. (Water Futures and Solutions (WFaS)*, n.d.), this might increase to the range fifty-five to sixty hundred km^3/year by 2050. As per the UN data, the agricultural sector, industries and municipalities share about 69, 19 and 12% of total fresh water, respectively, *(Water Scarcity | UNICEF*, n.d.). The above data gives insight into, why fresh water should be used efficiently and sustainably.

Fresh water is contaminating rapidly because of dye discharge from the paper, textile, food processing and printing sectors (Amor

[a] Department of Chemistry, Sri Sai University, Palampur, 176061 India.
ranaashvinder@gmail.com
ranaashvinder2020@gmail.com

et al., 2019; P. Sharma, Prakash, Palai, *et al.*, 2022; Xia *et al.*, 2022), producing almost 8 lakh tonnes of dyes per year, with two thousand tonnes dyes coming from textile industries (Yaseen & Scholz, 2019). In dye effluent, major pollutants are acids, salts, salts, glues and auxiliaries, which are toxic, xenobiotic, mutagenic, teratogenic and carcinogenic (Kaushik *et al.*, 2021; Paul & Ahankari, 2023; Xia *et al.*, 2022) and responsible for various health hazards like skin irritations, eye burns, asthma, skin irritations and allergic conjunctivitis (Solayman *et al.*, 2023; Yaseen & Scholz, 2019). Due to the disruption of aquatic life and plant photosynthetic processes, dye wastewater is also posing a serious threat to both aquatic and terrestrial life (Lellis *et al.*, 2019). Even though we are aware of the negative impacts and also have country's laws and regulations, we nevertheless discard these dyes into the environment without any treatment. So, it is of the utmost necessary to treat these dyes before their discharge as per the international and national standards.

Nowadays, numerous water treatment techniques are available, such as membrane filtration (Costa *et al.*, 2023), electrolysis (W. Zhang *et al.*, 2023), distillation (Hsu *et al.*, 2023), advanced oxidation process (H. Wang *et al.*, 2023), precipitation(Piaskowski *et al.*, 2018), ion exchange (P. Kumari *et al.*, 2023), flocculation (Sultana & Usman, 2023), and bio (Zain *et al.*, 2023)/synthetic (Taher *et al.*, 2023)-materials based adsorption. Among them, the adsorption technique is best, as it is a simple, effective and chemical-free approach. The evaporation, distillation and electrolysis processes are comparatively costly and also have a low rate of freshwater outflow. Membrane-based technology, i.e., reverse osmosis, which nowadays accounts for 69 % of the desalination plants globally, is also facing certain challenges such as high operating pressure requirements (10-80 bar) and membrane fouling problems (Chu *et al.*, 2021; Piaskowski *et al.*, 2018). The advanced oxidation process is costly as it requires energy and chemical reagents. Both biomaterials and synthetic-materials-based adsorbents and membrane filtration system work primarily on adsorption. The bio- based hydrogels in this field are gaining a huge amount of interest because of their highly porous, lightweight, eco-friendly nature and large specific area (Lin *et al.*, 2022; Malik *et al.*, 2023).

Recently, numerous polysaccharides including starch, alginate, chitosan, cellulose, etc., have been used to create environmentally benign and sustainable hydrogels (Barbucci *et al.*, 2003; Chaudhary *et al.*, 2021; S. Thakur, Chaudhary, *et al.*, 2022; S. Thakur, Verma, *et al.*, 2022). The high mechanical toughness, porous character, bio-degradable nature and flexibility of polysaccharides-based hydrogels make them a special candidate for the removal of contaminants from waste water (Pooresmaeil & Namazi, 2020). These bio-based polymers can adsorb contaminants without dispersing in water in numerous ways such as hydrogen bonding, van der Waals attraction, electrostatic contact and pi-pi attraction.

Cellulose is one of the major bio-degradable biopolymers available on earth and has been utilized in its various forms such as macro, micro and nano forms in numerous fields, such as in water purification i.e., pesticide adsorption (Rana, Mishra, *et al.*, 2021), water desalination (Rana, Gupta, *et al.*, 2021), dye removal and heavy metals adsorption (Rana, Scarpa, *et al.*, 2022), electronic industries (Rana, Guleria, *et al.*, 2022), air purification (Rana *et al.*, 2023) bio-chemical extraction (Rana, 2022; Singha & Rana, 2012), etc. (Rana, 2022; Singha & Rana, 2012; M. K. Thakur *et al.*, 2014). Out of various forms, nanocellulose (NC), due to its high surface area, amazing mechanical strength, and availability of abundant hydroxyl groups, has provided appealing results in diverse fields, most especially in the treatment of water (Rana, Gupta, *et al.*, 2021; Rana, Mishra, *et al.*, 2021; Rana, Scarpa, *et al.*, 2022).

Keeping in view the alluring characteristics of NC, the present review article has been focused on recent techniques employed for the synthesis of different NCs- i.e., cellulose nano crystals (CNCs), cellulose nanofibers (CNFs) and bacterial nanocellulose (BNC)based hydrogels and on evaluation of their potential in the removal of dyes from waste water (Fig. 1). In contrast to the previously published review articles(Ahmad *et al.*, 2023; Paul & Ahankari, 2023), none of which have been focused in particular on the dye adsorption potential of NC-based hydrogels, this article presents an updated and critical evaluation of recent findings on NC based hydrogels for adsorption of dyes from waste water. In addition, recent surface functionalization techniques employed or organic/inorganic additives added to NC hydrogels for tailoring the surface chemistry toward the effective removal of dyes have also been thoroughly reviewed.

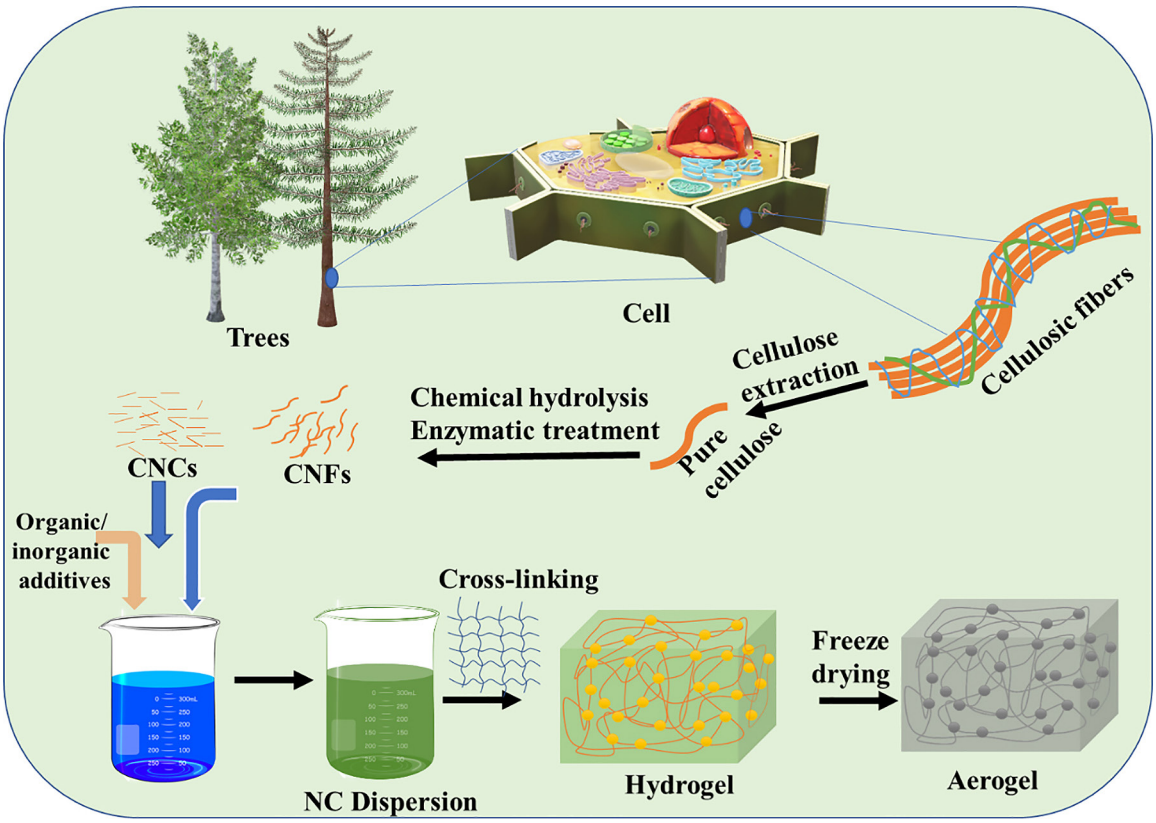

Figure 1. Schematic view of extraction of NC from plants and its conversion into hydrogel.

1.1. Why NC-based adsorbents are better than inorganic-based adsorbents?

The NC- based hydrogels possess superior or almost similar adsorbent capacity to that of inorganic or other adsorbents like carbon nanotubes, iron oxide, titanium dioxide, silicon dioxide, zinc oxide, fullerenes, etc. (Kaushik *et al.*, 2023). Additionally, their use also minimizes the safety issues that are typically associated with long-term use of inorganic materials and carbon nanoparticles(Lu & Astruc, 2020; P. Sharma, Prakash, & Kaushal, 2022; P. Sharma *et al.*, 2023). The separation of the powdered inorganic adsorbents from treated water and adsorption of pollutants at ppb levels are some of the great challenges. NCs based hydrogels are generally preferred over the other hydrogels, since they are more environmentally friendly, possess very large specific areas (depending upon drying methods and dimensions of cellulose fibers, highly flexible and mechanically tougher than other types of aerogels and their porosity and density can be easily controlled and theoretically predicted (Bhatnagar *et al.*, 2015; Mahfoudhi & Boufi, 2017).

1.2. Brief introduction about cellulose nanofibers, cellulose nano crystals and bacterial nanocellulose

NC can be classified into three types, namely CNCs, CNFs and BNC. The former two are obtained from plant wastes through chemical/enzymatic treatments; however, the latter one is produced by a wide variety of bacterial genera (Rana, Gupta, *et al.*, 2021). CNCs are rod shaped, highly crystalline and are generally extracted/synthesised from dried biomass by enzymatic hydrolysis or chemical hydrolysis techniques (Rana, Frollini, *et al.*, 2021). The chemical technique involves the utility of organic acid (citric/oxalic/acetic acid), inorganic acid (sulphuric acid, phosphoric, hydrochloric acid, etc.) or a combination of both at elevated temperatures (Rana, Frollini, *et al.*, 2021) (Fig. 1). Amorphous segments are eliminated during hydrolysis, leaving behind highly crystalline CNCs. The type of extraction procedure used affects the mechanical strength, thermal strength, aspect ratio, and hydrophilicity of CNCs. They typically have high thermal stability (T_{onset}: 300°C approx..) (Yin *et al.*,

2020) and tensile strength (700-7500 MPa) (Rana, Frollini, *et al.*, 2021), and possess low aspect ratio (13.9 ± 2.6) (Q. Wu *et al.*, 2017) (width: 1−50 nm and length:100-500 nm) (Rana, Frollini, *et al.*, 2021), Zeta potential of -44.40±4.12 mV and polydispersity index in range 22.32-23.58 (Fotie *et al.*, 2017). For the extraction of CNFs, the most popular methods are ultrasonication, grinding, high-pressure homogenization and microfluidization (Rana, Frollini, *et al.*, 2021). In comparison to CNCs, CNFs (diameter<100nm; length lies in micro-scale; aspect ratio 30-300) possess higher aspect ratio and low thermal stability (T_{onset}: 269.74°C), % crystallinity (45-80%), tensile strength (357.5 MPa) and zeta potential value (-55mV) (Radakisnin *et al.*, 2020; A. Sharma *et al.*, 2021). BNC is the purest form and has a structure like a twisted ribbon (diameter: 20 -60 nm; length in micrometer). It is synthesized by bacteria via a coupled polymerization and crystallization process (Jedrzejczak-Krzepkowska *et al.*, 2016). BNC displays a higher zeta potential value: -53.6 ± 0.7, crystallinity index: 89 % approx., T_{onset}: 224°C and mechanical strength (2 GPa) (Shak *et al.*, 2018; Tshikovhi *et al.*, 2020; Vasconcelos *et al.*, 2017).

2. GENERAL OVERVIEW OF SYNTHESIS OF NANOCELLULOSE-BASED HYDROGELS

Hydrogels are synthesized either through non-covalent or through covalent cross-linking pathways (Fig 2; Table 1) (Gulrez *et al.*, 2011; Kayra & Aytekin, 2018; Zainal *et al.*, 2021). The degree and type of cross-linking do not only affect the hydrogel formation but also the hydrogel's pore size, surface properties, porosity and overall network distribution (Al-Sabah *et al.*, 2019). Covalently cross-linked hydrogels mostly possess better mechanical toughness than their counterparts. However, the toxicity of cross-linking agents must be investigated before its utility, as a result, hydrogels may contaminate the water during water treatment. For this reason, efforts are generally made to prepare and utilize the cross-linking agent-free hydrogels. An example of such kind of hydrogel is the blended mixture of TEMPO-oxidized CNFs (TO-CNFs) and cationic guar gum, in which cross-linking takes place through the electrostatic interactions between carboxylate and ammonium groups (Dai *et al.*, 2019). Various methods utilized so far for the synthesis of NC-based hydrogels have been discussed in subsequent subsections.

2.1. Chemically cross-linked hydrogels

In the chemical approach, NC is graft copolymerized/modified and/or subjected to one-pot cross-linking. They are formed by the covalent linkage of -COOH, -OH, or other functional groups available on NC surface with the carboxyl, amide and amine groups of cross-linking agents. The cross-linking reactions are generally carried out through esterification, Schiff base linkage, Michael Addition reaction, epoxide linkage, etc. The most commonly utilized cross-linking agents are citric acid (CA) (Nasution *et al.*, 2022), glutaraldehyde (GA) (Chen *et al.*, 2022), epichlorohydrin (EPH) (El Bouazzaoui *et al.*, 2022; S. Huang *et al.*, 2019), N,N′-methylene bisacrylamide (MBA) (Cai *et al.*, 2020), succinic acid/succinic anhydride (ScA) (Z. Zhang, Abidi, *et al.*, 2022), tannic acid (TA) (Z. Zhang, Abidi, *et al.*, 2022) and divinyl sulfone (DS) (Kang *et al.*, 2016).

The NC can be directly converted into a hydrogel through one-pot cross-linking techniques, which involve conversion of NC into sol by dissolving in suitable solvents and then cross-linking it with suitable cross-linkers. Further, it can be graft copolymerized with some hydrophilic monomers or modified before crosslinking. Depending upon the types of monomers used, the NC-based hydrogels can be classified into three types, namely, homopolymer hydrogels, copolymer hydrogels and multi-polymer hydrogels. The homopolymer hydrogel involves the repetition of the single unit (Jawaid & Mohammad, 2017), and is formed by irradiation with high energy radiations or by dissolving in aqueous solution of NaOH/urea and subsequent cross-linking with epichlorohydrin (El Bouazzaoui *et al.*, 2022). Copolymer hydrogels are formed by using the binary monomer mixtures along with NC. Cai *et al.* (Cai *et al.*, 2020) prepared such kinds of hydrogels by binary monomer mixtures graft copolymerization of acrylic acid (AA) and acrylamide (AAm) monomers onto CNFs - TiO_2 mixtures using MBA as crosslinkers. Multipolymer hydrogels are made up (S. Huang *et al.*, 2019; Mohite & Adhav, 2017) by two independent cross-linked synthetic polymers and/or natural polymer components.

The polymerization of monomers can be carried out either through radical or ionic pathways. In radical polymerization, a polymer chain is generated by initially adding a redox chemical initiator or by using photo initiator to create a reactive center on the polymeric backbone, and then subsequently developing a new reactive center through reactions of

Factors / parameters	Physical crosslinked hydrogel	Chemical crosslinked hydrogel
Stability	Not very stable. Stability varies with pH, concentration and temperature.	Show better thermal, mechanical and structural stability.
Type of interaction forces	Non covalent forces such as hydrogen bonding, electrostatic interactions, hydrophobic interactions, or van der Waals interactions.	Involves covalent bonding between the chains.
Response to stress	Physically cross-linkages are typically weaker, and show reversible responses to stress.	Show irreversible response.
Solubility	Dissolve in organic solvents and water upon increase in temperature.	Do not dissolve in the surrounding environment.
Methods of formation	Heating/cooling polymerization, hydrogen bonding, freeze-thawing, photo-initiator, inverse emulsion technique, heat-induced aggregation, etc.	Chemical crosslinking between NCs can be made by using cross-linking agents or by reaction between the functionalized NCs or by reaction of a polymer chain with OH and COOH groups of NCs, establishing amide or ester linkage.
Cross-linkers types	Carbonates, sulfates, phosphates, and citrates or anions of Ca (II), Al (III), Fe (III), etc.	Citric acid, glutaraldehyde, epichlorohydrin, etc.
Lifespan	Shorter life span (from few days to a month)	Comparatively longer lifespan
Applications	Drug delivery, wound healing/dressing, controllable scaffolds, conventional filtration, etc.	Food/drugs packing, reinforcing agent, thermal protective equipment, medical or packaging application, biomedical and tissue engineering, biomedical devices, etc.
Toxicity	These hydrogels are safer for clinical purposes	Covalent cross-linking agents are usually toxic. So, there is a need to evaluate the toxicity of crosslinkers prior to the use of hydrogels for clinical purposes.

Table 1. Differences between physical and chemical crosslinking (Gulrez *et al.,* 2011; Kayra & Aytekin, 2018; Zainal *et al.,* 2021).

reactive sites with monomers. The chemical initiator technique has been adopted by a couple of researchers to develop NC-based hydrogels (Rao *et al.*, 2017; Zubik *et al.*, 2017). Zubik *et al.* (Zubik *et al.*, 2017) prepared thermo-Responsive poly(N-isopropylacrylamide)-CNCs and Rao *et al.* (Rao *et al.*, 2017) synthesized pH-responsive poly(acrylamidoglycolic acid)/CNC hybrid hydrogels through redox free radical polymerization technique. Vakili *et al.* (Vakili *et al.*, 2021) grafted poly (AA) onto CNCs to design a mucoadhesive hydrogel for the delivery of cisplatin to colorectal cancer. Zhao *et al.* (Zhao *et al.*, 2021) utilize a photoinitiator to crosslink methacrylate functionalized CNF with methacrylate hydroxyapatite. The resulting hydrogel composites demonstrated better mechanical strength (compressive strength: 0.198 MPa - 0.009 MPa) and reparability.

Depending upon the network charge, hydrogels may be broadly classified into ionic and non-ionic. NC-based ionic (anionic) hydrogels undergo cross-linking with an ionic unit with the help of a crosslinking agent. The best example of cationic hydrogel is chitosan, which is extracted from partial de-acetylation of chitin. The chitosan and cellulose behave differently at low pH. Between these, chitosan undergoes breakage of the chain at lower pH and thus shows good swelling at low pH (Poornachandhra *et al.*, 2023). Further, to enhance the hydrogel properties in addition to grafting/cross-linking, blending techniques have also been employed.

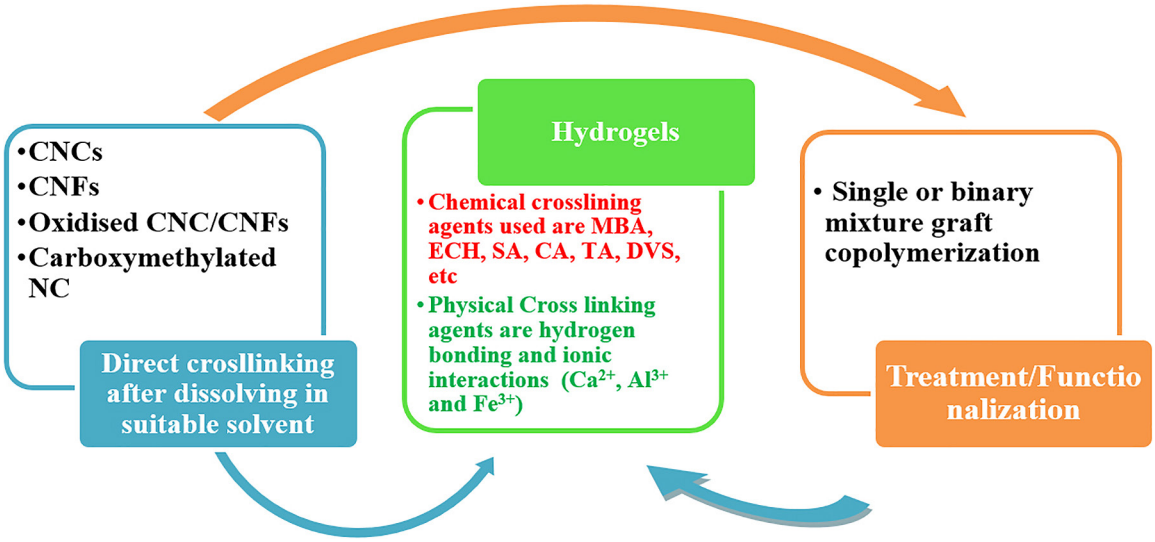

Figure 2. Possible ways for converting NC into NC-based hydrogels.

2.1. Physical cross-linking

Physical cross-linking is reversible and here polymer chains are held together by the physical entanglement of chains, van der Waals interactions, hydrogen bonding, ionic and electrostatic interactions or through other non-covalent interactions (Akhtar *et al.*, 2016; Bhaladhare & Das, 2022; Mohammadinejad *et al.*, 2019) (Fig. 3). Since there is no need to have a cross-linking agent, this technique is bio-compatible, safer and easy to process.

Xue *et al.* (Xue *et al.*, 2023) developed physically crosslinked TEMPO oxidized CNCs(TO-CNCs) beads by dropping solidification method, which involves dispersing a homogenous mixture of TO-CNCs in calcium chloride solution. The homogenous mixture, when comes into contact with calcium chloride solution, immediately solidifies and forms beads, which are subsequently freeze-dried before their utility for dye removal or FTIR characterization. Poornachandhra *et al.* (Poornachandhra *et al.*, 2023) synthesized NCC-Chitosan (CS) hydrogel beads by electrostatic interaction between -ve charged S-NCC and a positively charged CS. They dripped the homogenous mixture of NCC and CS, in alkali solution for solidification purposes or for the formation of hydrogel beads. The beads were further used for the removal of cationic dyes. Physically cross-linked hydrogels are frequently used for the adsorption of dyes or heavy metals from waste water due to their low sensitivity to pH, high porosity, and simplicity of regeneration with no loss of adsorption capacity (Sinha & Chakma, 2019).

3. FORMATION OF HYDROGELS

Akter *et al.* have accounted for six ways of cellulose hydrogel formation under the heading physical path of cross-linking. These include freeze-thaw, self-assembling, instantaneous gelation, inverse emulsion technique, reconstitution and ionotropic gelation(Akter *et al.*, 2021). However, chemical-cross linking can be carried out through graft copolymerization or polymerisation, chemical reactions, or through irradiations.

The most commonly used techniques for the preparation of NC hydrogels are the sol-gel method (Long *et al.*, 2018), emulsion polymerization (Y. Li *et al.*, 2022), self-assembly, graft copolymerization, chemical reactions, and 3-D printing techniques. Out of various techniques, the sol-gel method is simple and most commonly used. However, in this technique, the synthesis time varies with the type of catalyst and solvent used and can last from a few hours to several days (Bokov *et al.*, 2021; Lim *et al.*, 2015). It is irreversible, carried out at low temperatures and form 3-D networks. This process is covered in three steps; formation of gel, aging and drying (M. Wang *et al.*, 2021). Initially, the sol is prepared by dispersing NC in a suitable solvent along with a catalyst, which is then subjected to gelation. In the gelatin stage, the interaction (hydrogen bonding, ionic interactions, chemical/physical bonding, etc.) between the hydrolyzed NC particles takes place and a 3D structured viscoelastic gel is formed. Further, the degree of crosslinking depends upon the NC

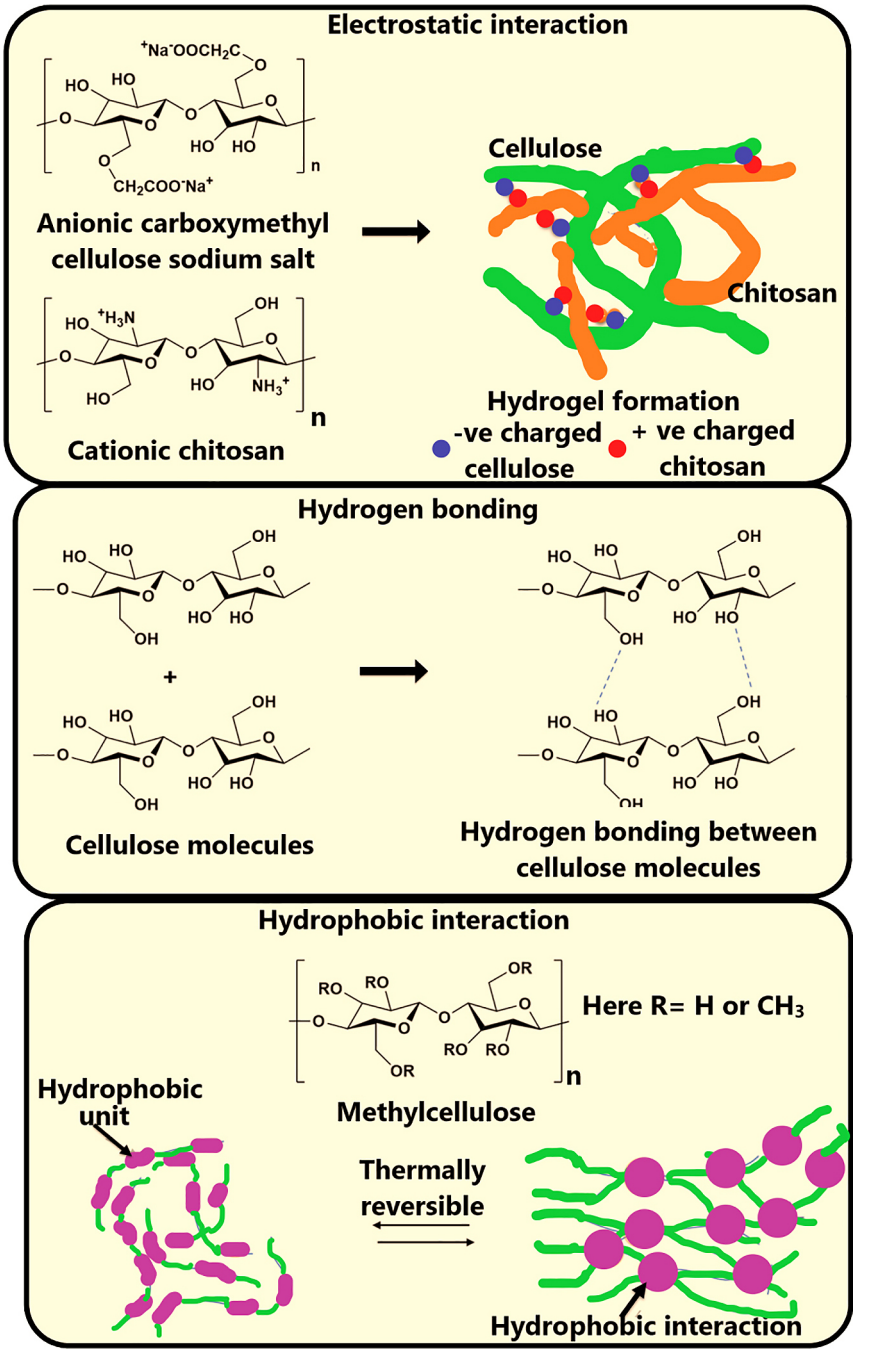

Figure 3. Mechanism for the formation of physical cross-linking between two different polysaccharides (Bhaladhare & Das, 2022) (Reproduced with permission from Ref. (Bhaladhare & Das, 2022) Copyright 2022, RSC)

concentration, as its higher concentration result in stiffer aerogel of low porosity (Long *et al.*, 2018). Li *et al.* (W. Li *et al.*, 2021) prepared mesoporous NC/sodium alginate (SA)/ CMC using this technique (Fig. 4). They initially ultrasonicated the mixture of TO-CNF, SA and CMC in distilled water for 30 minutes to obtain a viscous solution and subsequently dropped it into a calcium chloride solution for coagulation purposes. The obtained aerogel beads after dipping in water and washing with ethanol were transferred to tert-butanol and subsequently freeze-dried.

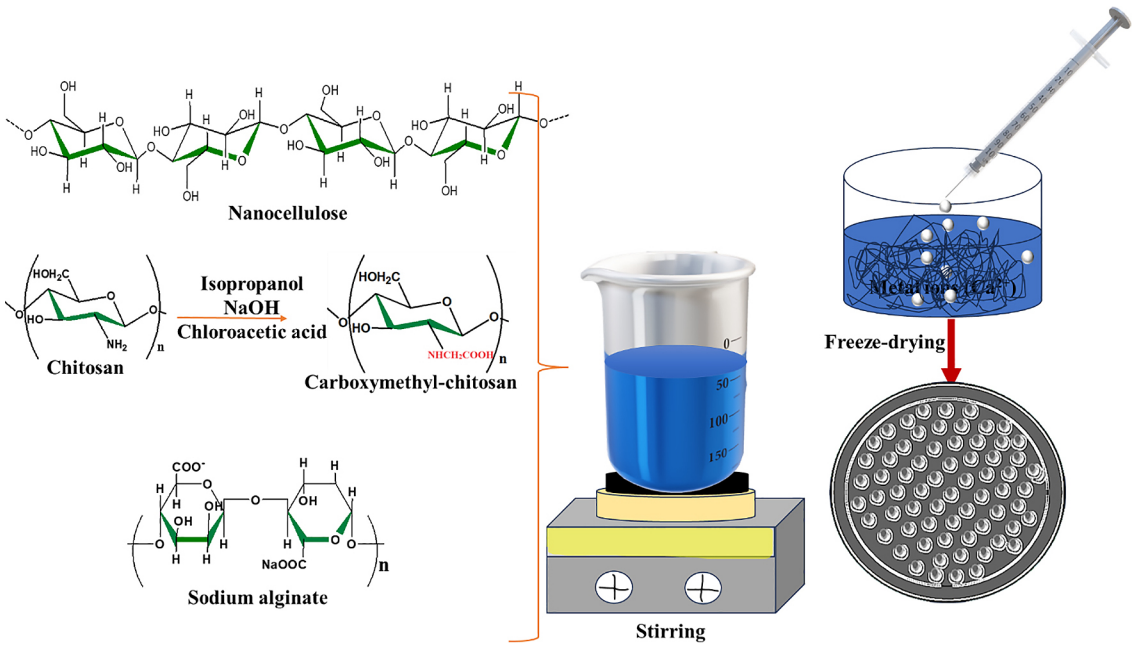

Figure 4. Hydrogel beads synthesis through the sol-gel technique (W. Li *et al.*, 2021) (Reprinted with permission from Ref. (W. Li *et al.*, 2021) Copyright 2021, Elsevier)

Emulsion polymerization is comparatively less time-consuming but it requires the centrifugation process for separation purposes (Y. Li *et al.*, 2022) (Fig. 5). Recently, a self-assembly technique has been employed by Berglund *et al.* (Berglund *et al.*, 2023), for developing CNF-based hydrogels (Fig. 6). They used two different approaches, i.e., vacuum-assisted filtration (VF) and evaporation through suspension casting (SC) for the removal of water and for CNFs hydrogel self-assembly. The hydrogel formed through the casting technique showed a less intertwined/interconnected layered structure after swelling and thus demonstrated three times higher water absorption capability than its counterpart (Fig. 6). Zhang *et al.* (X. Zhang *et al.*, 2023) also used a self-assembly approach to fabricate CNFs/montmorillonite/polyethyleneimine (cross-linkers) hydrogels adsorbent for the removal of copper and methylene from aqueous solutions. The existence of hydrogen bonding and electrostatic interactions has been confirmed through FT-IR results. Partially deacetylated chitin and TO-CNFs were physically cross-linked through self-assembly technique resulting in Chitin/TOCNFs biohybrid hydrogels (X. Zhang *et al.*, 2019). The process was carried out at room temperature without any use of cross-linker and the developed hydrogel after freeze-drying displayed a highly porous structure. Nguyen *et al.* (Nguyen *et al.*, 2022) have prepared CNF/GO hydrogels by thoroughly mixing and ultrasonicating the mixture of CNFs-GO and subsequently freeze-drying it. The developed aerogel was reported to be mechanically tougher and showed dye adsorption tendency greater than 90% even after the fifth consecutive recycle. Ching *et al.* (Ching *et al.*, 2018) used ultrasonication technique to convert microcellulose into NC hydrogels, which were subsequently freeze-dried and carbonised in a nitrogen atmosphere to produce highly porous carbon. Hosseinzadeh and co-authors (Hosseinzadeh *et al.*, 2019) synthesised CNC-g-poly[AA-co- 2-hyderoxy ethyl methacrylate (HEMA)] hydrogels through graft copolymerization process utilizing MBA as a cross-linker and APS as initiator. The synthesised hydrogel was treated with ethanol for water removal purposes and subsequently dried in vacuum for further application in water purification.

4. DRYING OF HYDROGEL

After the formation of a hydrogel, the solvent is removed by employing freeze-drying (FD), vacuum drying (VD), critical point drying (CPD) or ambient pressure drying (APD) and freeze-casting techniques. The drying process controls the pore size, morphology, surface area and density of the resulting aerogel (Guastaferro *et al.*, 2021). Based on the pore size and density, the aerogels developed

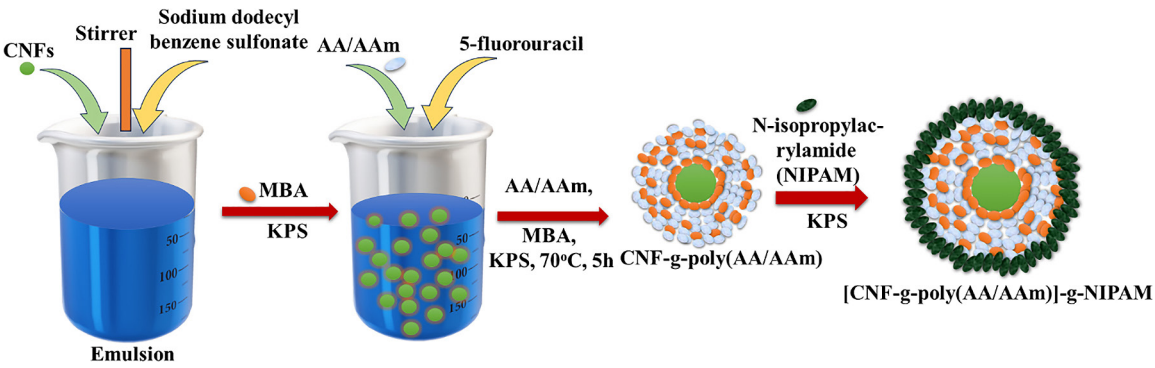

Figure 5. Hydrogel formation through emulsion polymerization technique (Y. Li *et al.,* 2022). [Adopted from Ref. (Y. Li *et al.,* 2022)].

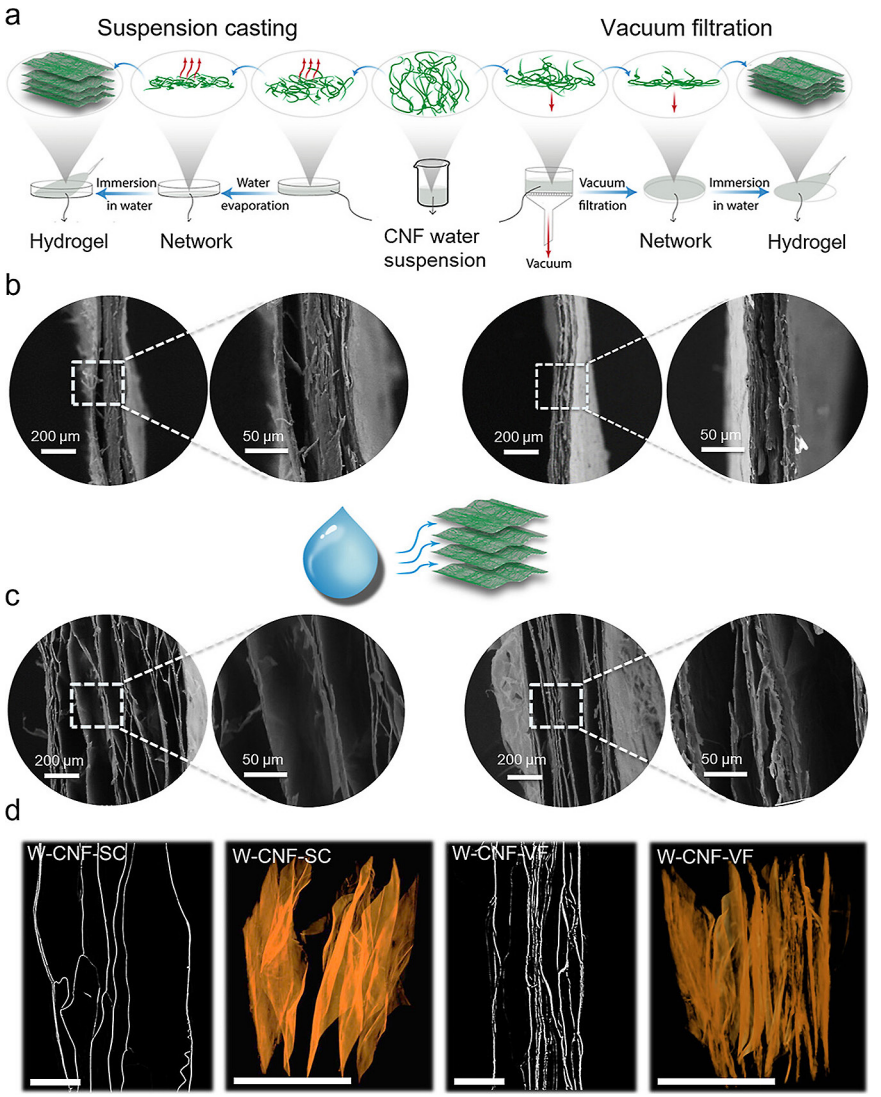

Figure 6. (a) CNF hydrogel self-assembly set up via SC and VF techniques, SEM images of freeze dried hydrogels (b) before absorption and (c) after absorption, and (d) their visualization through 2D and 3D X-ray microtomography (XRT) reconstruction after 1000% absorption (Berglund *et al.,* 2023). (Reprinted from Ref. (Berglund *et al.,* 2023) Copyright 2023, ACS under CC BY 4.0).

from CPD, APD and FD have been named as aerogel, xerogel and cryogel, respectively (Aegerter *et al.*, 2011; Paul & Ahankari, 2023). Further, because of their high absorption potential, these hydrogels have been widely used for absorption/adsorption of dyes from waste water. Among different drying techniques, the FD is generally preferred as it forms aerogels of suitable pore size and strength, whereas in the case of CPD and APD the aerogels of low porosity are formed (Paul & Ahankari, 2023)]. Couple of researchers have also reported better pore size for VD aerogels in comparison to FS aerogels.

In FD technique (low pressure and low temperature), the aqueous gel is initially frozen by employing liquid N_2/dry ice/ refrigerator and then dried in a vacuum oven. It has a disadvantage that during crystal growth, some cracks may be formed and shrinkage can be seen in the structure (Hammami & René, 1997; P. Wu *et al.*, 2019). The VD technique involves sublimation of a sample directly in vacuum. This technique is a more cost-effective and easily affordable approach than FD. Also, FD requires a combination of a refrigeration system, a condenser and a vacuum for removing moisture, whereas no such equipment is required in VD. CPD is done at critical pressure and temperature of solvent and it has the advantageous that at the critical state the capillary forces, because of the free movement of molecules, can be avoided. In both FD and CPD techniques (CPD requires high temperature and pressure and it is time-consuming), the aqueous phase in the hydrogel is replaced with gas (air); however, their respective pathway is different (De France *et al.*, 2017; Gurav *et al.*, 2010).

Freeze casting, just like FD, is another alluring technique, which, contrary to the latter one, forms anisotropic hydrogels (Chau *et al.*, 2016; De France *et al.*, 2017). Chau *et al.* (Chau *et al.*, 2016) have synthesized such kinds of hydrogels with controllable pore size from aldehyde-functionalized CNCs and hydrazide-functionalized poly(oligoethylene glycol methacrylate) (POEGMA) through directional freeze-casting. The pore morphologies were noticed to vary with the total mass of CNCs and the relative ratio of CNC and POEGMA. APD is the most efficient approach in terms of time and cost. However, when liquids are evaporated at ambient pressure, the capillary stress at the liquid-vapor interface causes the gel to contract and thus reduces its porosity (Zuo *et al.*, 2015). Further, due to the exceptional benefits i.e., low cost and sustainability, the FD is still the most frequently utilized drying technique for developing NC aerogels.

5. REMOVAL OF DYES FROM WASTE WATER

NC hydrogels-based adsorbents can be broadly classified into five categories i.e., virgin NC adsorbents, biopolymer blended NC hydrogels, inorganic materials blended NC hydrogels, functionalized NC hydrogels and metal/metal oxide doped NC-based hydrogels. All of these types of adsorbents have been successfully used for the removal of different dyes from contaminated water (Table 2). For removal of methylene blue (MB), the different types of adsorbents used were sulphuric acid extracted-NC/carboxymethyl cellulose (CMC)/SA hydrogels (Yap *et al.*, 2023), TO-CNFs beads (Xue *et al.*, 2023), CNCs-chitosan (CS) hydrogel (Poornachandhra *et al.*, 2023), carbonized hydrogels (Ching *et al.*, 2018), CNFs-graphene oxide (GO) hydrogel (Nguyen *et al.*, 2022; Shandong Agricultural University *et al.*, 2019; Z. Wang *et al.*, 2021), CNFs/poly (ethylene imine)PEI/Ag composite aerogel (W. Zhang *et al.*, 2020) (adsorption plus dye decolouration), CNF/montmorillonite nanosheet (MMT)/PEI hydrogel (X. Zhang *et al.*, 2023), CNCs-SiO_2 (Ruan *et al.*, 2022), NC-UIO-66 (Z. Wang *et al.*, 2019), metal-organic frameworks (MOF)-199@Carboxylated CNC/Carboxymethyl CS (CMCS) (Jiang *et al.*, 2022), CMC/carboxylated-CNFs (T. Zhang *et al.*, 2022), TO-CNFs/partially deacetylated chitin hydrogels (X. Zhang *et al.*, 2019), Sago pitch waste extracted CNFs (Beh *et al.*, 2020), BNC/MoS_2 hybrid hydrogels (Ferreira-Neto *et al.*, 2020), PVA/lignin rich NC-soluble ash -MMT hydrogels (R. Huang *et al.*, 2023), spherical NC-g-poly 2-acrylamido-2-methylpropane sulphonic acid [poly(AMPSA)] hydrogel (Jamwal *et al.*, 2023), SA/GO/CNC 3D scaffold (Al-Shemy *et al.*, 2022), and SA-electrostatically stabilized CNCs (Tavakolian *et al.*, 2020). Among different adsorbents, the best results were obtained with MOF-199@Carboxylated CNC/CMCS adsorbents [maximum adsorption capacity (q_m):1112.2mg/g] (Jiang *et al.*, 2022). Further, for methyl orange (MO) dye removal, out of various types of adsorbents like Poly([2-(acryloyloxy)ethyl] trimethylammoniumchloride) [poly(AETAC]-g- 1 % TO-CNF hydrogels (Roa *et al.*, 2021), poly(2-(dimethylamino) ethyl methacrylate) [poly(DMAEMA))/NC hydrogels (Safavi-Mirmahalleh *et al.*, 2020), poly(DMAEMA)/ (3 -amino)propyltriethoxysilane (AMPES)-CNCs (Safavi-Mirmahalleh *et al.*, 2020), poly (DMAEMA)/hexadecyltrimethoxysilane

 https://doi.org/10.37819/nanofab.8.1757

Hydrogel name	Drying conditions	Dye	Optimized parameters	q_m in mg/g	% Removal efficiency (RE)	Number of time regenerated and % RE after regeneration	Adsorption isotherm/ Kinetic data	Ref
TO-NC/CMC/SA	Freeze-dried	MB	Time: 4 hr; Adsorbent: 4mg; MB concentration: 50 mL solution of 10 ppm conc.; Condition: immersion	109.03	93.7	—		(Yap *et al.*, 2023)
Poly(AETAC)-g-TO-CNF hydrogels	Freeze-dried	MO	Time: 5 hr; pH: 7.64, Adsorbent: 50mg; adsorbate concentration: 40 mL of 2000 mg/L) concentration; Condition: immersion	1379	96	5 times; After the fifth cycle; q_e was noted to be 5% of the original value	Pseudo second order kinetic	(Roa *et al.*, 2021)
TO-CNFs beads	Freeze-dried	MB	Time: 50 min; pH: 9, Adsorbent: 50 mg; adsorbate concentration: 5 mmol/L) concentration; Condition: immersion	682	80% for 5 mmol/L MB and >90% for 1 mmol/L MB concentration	Showed 83% RE for MB even after 5 cycles, when HCl was utilized as an eluting agent	Langmuir isotherm model; second-order kinetics	(Xue *et al.*, 2023)
Dialdehyde-CNC/PVAm hydrogel	Freeze dried	CR,	Time: 8 hr; pH: 3.5, Adsorbent: 0.5 g/L; adsorbate concentration: 100 mg/L) concentration; Condition: immersion	869.1	99.9		Sips model / Pseudo second order kinetics, indicating chemisorption of dyes	(Jin *et al.*, 2015)
		AR GR		1469.7	99.9			
		reactive light yellow K-4G		1250.9	99.9			
Poly(DMAEMA)/ NC hydrogels	Freeze drying	MO	Time: 144 min; pH: 1, Adsorbent: 0.5 g/L; adsorbate concentration: 5 mg/ L, 100 mL; ambient temperature; Condition: immersion	0.75 approx.	—		Pseudo-first-order model	(Safavi-Mirmahalleh *et al.*, 2020)
Poly(DMAEMA)/ AMPES-CNCs		MO		0.6	—		Pseudo-first-order model	

Hydrogel name	Drying conditions	Dye	Optimized parameters	q_m in mg/g	% Removal efficiency (RE)	Number of time regenerated and % RE after regeneration	Adsorption isotherm/ Kinetic data	Ref
Nanobentonite/ NC/CS aerogel	Lyophilised/ freeze-dried	BB	Time: 40 min; pH: 2, Adsorbent: 5 mg; adsorbate concentration: 4000 mg/L, 5 mL; temp: 313 K; Condition: immersion	29.842 g/g	—		Sips isotherm/ pseudo-first-order	(V. Sharma *et al.*, 2020)
	Lyophilised/ freeze dried	DB	Time: 60 min; pH: 4, Adsorbent: 5 mg; adsorbate concentration: 4000 mg/L, 5 ml ; temp: 323 K; Condition: immersion	20.927 g/g	—		Sips isotherm/ pseudo second order	(V. Sharma *et al.*, 2020)
P(AA-co-HEMA)-g-CNC	Ethanol washes and vacuum dried	CV	Time: 150 min; pH: 12, Adsorbent: 1.6 mg; adsorbate concentration: 50-200mg/L, 50 ml; temp: 55°C; Condition: immersion	231	—	First regeneration cycle: 90 mg/g and after the fifth cycle: 71 mg /g at pH 9.0.	—	(Hosseinzadeh *et al.*, 2019)
CNC-CS hydrogels	Hot air oven	CV	Time: 60 min; pH: 9, Adsorbent: 0.5 gm; adsorbate concentration: 60mg/L, 25 mL; temp: 25°C; Condition: immersion	14.87	94.75	Retained RE of 60% after 7-8 cycle	Langmuir and Freundlich model/pseudo-second model	(Poornachandhra *et al.*, 2023)
		MB	Time: 60 min; pH: 9, Adsorbent: 0.13 gm; adsorbate concentration: 30mg/L, 25 mL; temp: 25°C; Condition: immersion	14.72	95.88	Retained RE of 82% after 3rd cycle	D-R and Freundlich model/pseudo-second model	(Poornachandhra *et al.*, 2023)
Freeze dried NC after carbonization at 800°C	Carbonized hydrogel	MB	Time: 10 min; Adsorbent: 50 mg; adsorbate concentration: 10mg/L, 50 mL; Condition: immersion	98	98%	—	—	(Ching *et al.*, 2018)

https://doi.org/10.37819/nanofab.8.1757

Hydrogel name	Drying conditions	Dye	Optimized parameters	q_m in mg/g	% Removal efficiency (RE)	Number of time regenerated and % RE after regeneration	Adsorption isotherm/ Kinetic data	Ref
CNFs/PEI/ Ag composite aerogel	Freeze dried	MB & CR	Time: 5 min in case of MB and 29 min in case of CR; Adsorbent aerogel of fixed size; adsorbate concentration: 10mg/L, 40 mL; $NaBH_4$: 10 mL, 50 mM; Condition: both Inflow and immersion	—	Approx. 98% discoloration efficiency	Retained its dye discoloration capability (98%) even after the 10 cycle	--	(W. Zhang *et al.*, 2020)
CNFs/GO aerogels	Freeze dried	MB	Time: 20 min; Adsorbent 0.1 gm; adsorbate concentration: 20mg/L, 50 mL; Room temperature; Condition: immersion	10.48	99	Showed a adsorption capacity of 90% after fifth cycle; The aerogel was stable after 30 compression cycles	Pseudo-second-order model	(Nguyen *et al.*, 2022)
CNF/MMT/PEI hydrogel	Freeze-dried	MB	Time: 24 hr; pH: 10; Adsorbent 30 mg; adsorbate concentration: varied 5-800 mg/L, 30 mL; Temperature: 45°C; Condition: immersion	147.6; 361.9 (calculated from Sips model)	73.8	After 5th cycle RE: 49.3%	Sips isotherm model/fractal-like pseudo-second-order	(X. Zhang *et al.*, 2023)
Cu-BTC/CNFs aerogel	Freeze-dried	CR	Time: 18 hr; Adsorbent 0.01 g; adsorbate concentration: varied 50 mg/L, 10 mL; Temperature: 25°C; Condition: immersion	39	—	—	Langmuir isotherm model/ Pseudo second-order kinetic	(Shaheed *et al.*, 2021)
CNFs/GO	Freeze-dried	MB	Time: 6 min; Adsorbent 20 mg; adsorbate concentration: 50 mg/L, 20 mL; Condition: immersion	111.2	98	After 3rd cycle RE:98%; q_m: 42.8	Langmuir adsorption isotherm/Pseudo-second-order kinetics	(Z. Wang *et al.*, 2021)
		TC		47.3	97	After 3rd cycle RE:97%; q_m: 28.5		
CNFs/GO	Freeze-dried	MB & CR	Time: 24 hr; adsorbate concentration: 10 mg/L, 300 mL; Room temperature; Condition: In flow	MB: 265.6; CR: 21.5	—	—	—	(Shandong Agricultural University *et al.*, 2019)

Hydrogel name	Drying conditions	Dye	Optimized parameters	q_m in mg/g	% Removal efficiency (RE)	Number of time regenerated and % RE after regeneration	Adsorption isotherm/ Kinetic data	Ref
NC/UIO-66	Freeze-dried	MO & MB	Time: 350 min; Adsorbent 20 mg; adsorbate concentration: 50 mg/l, 20 mL; pH: 7; Condition: immersion	71.7 & 51.8	—	After 4th cycle: 92% adsorption ability	Pseudo-second-order model	(Z. Wang *et al.*, 2019)
CNCs/SiO_2	Freeze-dried	MB	Time: 180 min; Adsorbent 10 mg; adsorbate concentration: 100 mg/l, 20 mL; pH: 10; temp: 298 K; Condition: immersion	190.85	Approx. 90% at 45mg adsorbent dosage	After 5 cycles: 60% adsorption rate	Langmuir isotherm model/ Pseudo-second order	(Ruan *et al.*, 2022)
Cu_2O/TiO_2/CNF/rGO	Freeze-dried	MO	Time: 120 min; adsorbate concentration: 20 mg/L, 50 ml; Room temperature; Condition: immersion	11.28	85.62%	After 4th cycle: 79.5% photodegradation rate	Pseudo-Second Order/Photodegradation was best suited to Langmuir-Hinselwood pseudo-first-order kinetics	(Zheng *et al.*, 2022)
MOF-199@ Carboxylated CNC/CMCS	Freeze-dried	MB	Time: 80 min; Adsorbent 6 mg; adsorbate concentration: 20 ml of 1000 mg/L; pH: 5.25; temp: 298 K; Condition: immersion	1112.2	—	—	Freundlich adsorption isoherm/ Pseudo-second-order kinetic model	(Jiang *et al.*, 2022)
CNC-PEI-beta-cyclodextrin/ poly(AAm) hydrogel	Freeze-dried	MO	Time: 200 min; Adsorbent 0.1gm; adsorbate concentration: 100 ml of 160mg/L; Condition: immersion	155.93	97.46	After 5 cycles: RE 76.67%	Langmuir isotherm model/ Pseudo-second-order kinetic model	(Q. Li *et al.*, 2021)
CMC/carboxylated-CNFs	Freeze-dried	MB	Time: 12 hr; Adsorbent 17 mg; adsorbate concentration: 100 ml of 100mg/L; temp: 30°C; Condition: immersion	579.50 mg/g; Through Langmuir model: 917.43 mg/g	90	After 5th cycle decreased to 513.2 mg/g	Langmuir isothermal model/ pseudo-second-order kinetic; Hydrogel did not collapse even after ten cycles	(T. Zhang *et al.*, 2022)

https://doi.org/10.37819/nanofab.8.1757

Hydrogel name	Drying conditions	Dye	Optimized parameters	q_m in mg/g	% Removal efficiency (RE)	Number of time regenerated and % RE after regeneration	Adsorption isotherm/ Kinetic data	Ref
TO-CNFs / partially deacetylated chitin hydrogels	Freeze-dried	MB	pH: 10; time: 24 hr, temp: 25°C; adsorbate concentration: 50 mg/L; Condition: immersion	303; Through Langmuir model: 531	—	After 5th cycle adsorption capacity decreased to 50%	Langmuir adsorption/both pseudo first and second order kinetics	(X. Zhang *et al.*, 2019)
Sago pitch waste extracted CNFs	Freeze dried	MB	Adsorbent dosage: 20 mg; Adsorbate dosage: 20 ml of 20 mg/L; pH 7; Room temperature; Condition: immersion	222.2	99	—	Langmuir isotherm model/ Pseudo-second-order kinetic model	(Beh *et al.*, 2020)
Bacterial NC/ MoS_2 hybrid hydrogels	CO_2 supercritical drying	MB	Adsorbate dosage; 60 ml of 5 gm/L; 30 min of pre-adesorption in the dark and 90 min of UV photocatalytic removal Condition: Inflow	—	96	After 6th cycle: approx. 86%	—	(Ferreira-Neto *et al.*, 2020)
PVA/lignin rich NC-soluble ash – MMT hydrogels	—	MB	Time: 6 hr; adsorbent dosage: 0.5 g; adsorbate dosage: 30 ml of 0.25 mg/mL; Temp:50°C; Condition: immersion	—	97.3	—	Pseudo-second-order	(R. Huang *et al.*, 2023)
Pinus wallichiana derived spherical NC-g-poly (AMPSA) hydrogel	Dried in oven	MG	Time: 60 min; pH: 6; adsorbent dosage: 10 mg; adsorbate dosage: 10 mL of 50-300 mg/L; Condition: immersion; Temp 30°C	292.62; Langmuir q_m: 357.143	91.7	After 8th cycle: approx. 60%	Langmuir isotherm model/ Pseudo-second order	(Jamwal *et al.*, 2023)
		MB	adsorbate dosage: 50mg/L	—	75	—	—	
		CV	adsorbate dosage: 50mg/L		66	—	—	
		RB	adsorbate dosage: 50mg/L		6			
		MO	adsorbate dosage: 50mg/L		4			

Hydrogel name	Drying conditions	Dye	Optimized parameters	q_m in mg/g	% Removal efficiency (RE)	Number of time regenerated and % RE after regeneration	Adsorption isotherm/ Kinetic data	Ref
Anionic dialdehyde partially fibrillated cellulose	Freeze-dried	Cationic dyes (BBY and BCB and CR) and anionic dyes (AR AG25, ABM and ARS)	Adsorbent dosage: 7.5 gm; adsorbate dosage: 15 ml of 25mg/L; Time: 5hr; pH:7; Temp: 25°C; Condition: immersion	129.6 against CR; showed better q_m towards cationic dyes	24.3 in in-flow condition		Langmuir isotherm model	(X. Huang *et al.*, 2023)
Cationic dialdehyde partially fibrillated cellulose-modified by Girad's reagent T			Adsorbent dosage: 7.5 gm; adsorbate dosage: 15 ml of 25mg/L; Time: 5hr; pH:7; Temp: 25°C; Condition: immersion	540.3 against CR; showed better q_m towards anionic dyes	97% in immersion and 48.7 in in-flow	After the 5th cycle: approx. 60%	Freundlich isotherm model	
SA/GO/CNC 3d scaffold	Freeze-dried	MB	Time: 600 min; pH:6; adsorbent: 2.5g/L; adsorbate dosage: 20 ml of 100mg/L; Temp: 25°C; Condition: immersion	49.75 approx.	90% approx..		Both Pseudo first and second-order	(Al-Shemy *et al.*, 2022)
PDA-CNFs-PEI hydrogels	Freeze-dried	MO	Time: 12 hr; Adsorbent dosage: 29.5 mg; adsorbate dosage: 40 ml of 200 mg/L; pH: 4; room temperature; Condition: immersion	265.9	Approx. 97%	After 4th cycle: 89%	Langmuir isothermal model/ pseudo 2nd order	(Tang *et al.*, 2019)
SA-electrostatically stabilized CNCs		MB	Time: 2 hr; Adsorbent dosage: 30 mg; adsorbate dosage: 25 ml of 800 mg/L; room temperature; Condition: immersion	549.7; However, at 6000 mg/L dye concentration: 1250	98%	After 3rd cycle falls from 150mg/g (approx.) to <115 mg/g; when dye conc. Was 3200mg/L	Pseudo-second order	(Tavakolian *et al.*, 2020)

Table 2. Data on the removal of dyes from waste water by using different kinds of NC based hydrogels.

https://doi.org/10.37819/nanofab.8.1757

Table 2. Data on the removal of dyes from waste water by using different kinds of NC based hydrogels.

(HMTS) -CNCs (Safavi-Mirmahalleh *et al.*, 2020), NC/UIO-66 (Z. Wang *et al.*, 2019), Cu_2O/TiO_2/CNF/reduced graphene hydrogel (rGO) (Zheng *et al.*, 2022), CNC-PEI-beta-cyclodextrin/poly(AAm) hydrogel (Q. Li *et al.*, 2021), NC-g-poly (AMPSA) (Jamwal *et al.*, 2023) and polydopamine (PDA)-CNFs-PEI hydrogels hydrogels (Tang *et al.*, 2019), the best result was shown by poly(AETAC)-g-TO-CNF hydrogels (q_m: 1379 mg/g) (Roa *et al.*, 2021). Efforts have been also made for removal of other dyes like congo red (CR)[adsorbents used were Dialdehyde-CNC/polyvinylamine (PVAm) hydrogel (Jin *et al.*, 2015), CNFs/ PEI/Ag aerogel (W. Zhang *et al.*, 2020), Cu-(benzene 1,3,5-tricarboxylic acid) BTC/CNFs aerogel (Shaheed *et al.*, 2021), CNFs/ GO (Shandong Agricultural University *et al.*, 2019) and anionic dialdehyde partially fibrillated cellulose (X. Huang *et al.*, 2023)], acid red GR (ARGR)[Dialdehyde-CNC/PVAm hydrogel] (Jin *et al.*, 2015) , acid green 25 (AG25) & acid brown M (ABM) [Anionic dialdehyde partially fibrillated cellulose] (X. Huang *et al.*, 2023), bromophenol blue (BB) & direct blue 6 (DB) [Nanobentonite / NC/CS aerogel] (V. Sharma *et al.*, 2020), crystal violet (CV) [poly(AA)-co-2-hydroxyethylmethacrylate HEMA-g-CNC (Hosseinzadeh *et al.*, 2019) and CNC-CS hydrogels (Poornachandhra *et al.*, 2023)], malachite green (MG)[NC-g-poly (AMPSA)] (Jamwal *et al.*, 2023); bismarck brown Y (BBY), brilliant cresyl blue (BCB) and alizarin red S (ARS) [Anionic dialdehyde partially fibrillated cellulose] (X. Huang *et al.*, 2023) and rose bengal (RB) [NC-g-poly (AMPSA)] (Jamwal *et al.*, 2023). The impact of various parameters has been discussed in subsequent sections.

6. MECHANISM OF DYE ADSORPTION/DEGRADATION

A proposed mechanism for interaction between different types of hydrogels and cationic/anionic dyes is given in Figure 7. Poornachandhra *et al.* (Poornachandhra *et al.*, 2023) during their study on the interaction of CNCs/CH hydrogels with cationic dye, reported that it may take place through five different ways, such as through hydrogen bonding, van der Waals forces, dipolar bonds, n-p, and electrostatic interaction. They further discussed the possibility of two types of hydrogen bonding, namely dipole-dipole hydrogen bonding, which takes place between hydrogen present in the hydroxyl group of hydrogel and the H-acceptor (nitrogen) in the cationic dye, and Yoshida H-bonding interaction, which occurs between the hydroxyl group of hydrogel and the aromatic rings of cationic dyes. Nguyen *et al.* (Nguyen *et al.*, 2022) reported the possibility of the existing Pi-Pi stacking interactions between NC/GO and the conjugated system of dyes (MB). Further, some researchers also loaded the NC with a photocatalyst, for dual functionality of hydrogels as dye adsorber and degrader (W. Zhang *et al.*, 2020; Zheng *et al.*, 2022). The mechanism of dye degradation using photo nanocatalyst loaded NC-based hydrogels is given in Figure 8. From the figure, we can see how different radicals are generated at the intermediate stage of the reaction and lead to the degradation of different dyes.

7. ADSORPTION KINETICS AND ISOTHERMAL STUDY

7.1. Adsorption kinetics

A lot of work has been done on the study of NC-based hydrogel adsorption system kinetics by employing time interval tests, which involve immersion of sample in the dye solution and measurement of dye concentration after its withdrawal at different time intervals. Lagergren's pseudo-first-order and Ho's pseudo-second-order models are the two main kinetic models that have been utilized to monitor the kinetics of adsorption of dyes onto NC hydrogels (Dąbrowski, 2001; Günay *et al.*, 2007) (Table 3). The kinetic of adsorption gives us an idea about possible mechanisms and helps in defining the rate-determining step during adsorption. This step is of the utmost importance as it helps in optimizing process parameters and setting up optimized parameters for the removal of dyes at an industrial scale (Febrianto *et al.*, 2009). If the pseudo-first-order model is found to be the best fit for experimental results, then it predicts physical adsorption. However, if the pseudo-second-order model fits well with the experimental data, then adsorption may be supposed to take place through the chemisorption pathway. Many phases have been identified in the adsorption process by making use of the intraparticle diffusion model, including rapid diffusion of adsorbate molecules over the external layer of the adsorbent; diffusion of adsorbate intraparticle in pores; the formation of chemical/physical bonds at the active centres on the adsorbent.

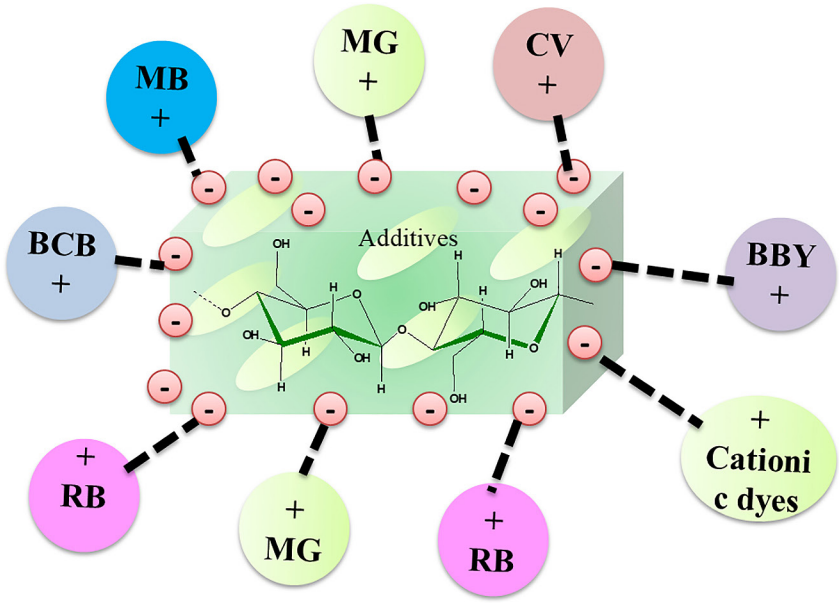

Here RB is rhodamine B
and -ve charge on hydrogel may be due to -O-, -COO- groups, etc

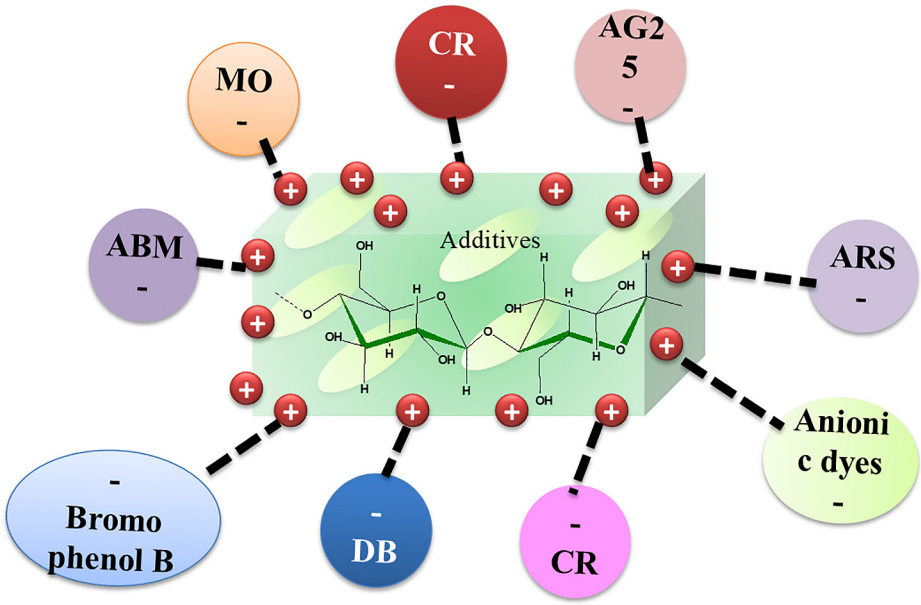

Here + ve charge on hydrogels may be due to the presence of
H_3O^+ and NH_3^+groups

Attraction may be electrostatic, hydrogen bonding, van der Waals, n-*Pi* and *Pi-Pi* stacking interactions

Figure 7. Schematic view of adsorption of (a) cationic dyes and (b) anionic dyes onto NC-based hydrogels (Poornachandhra *et al.*, 2023).

 https://doi.org/10.37819/nanofab.8.1757

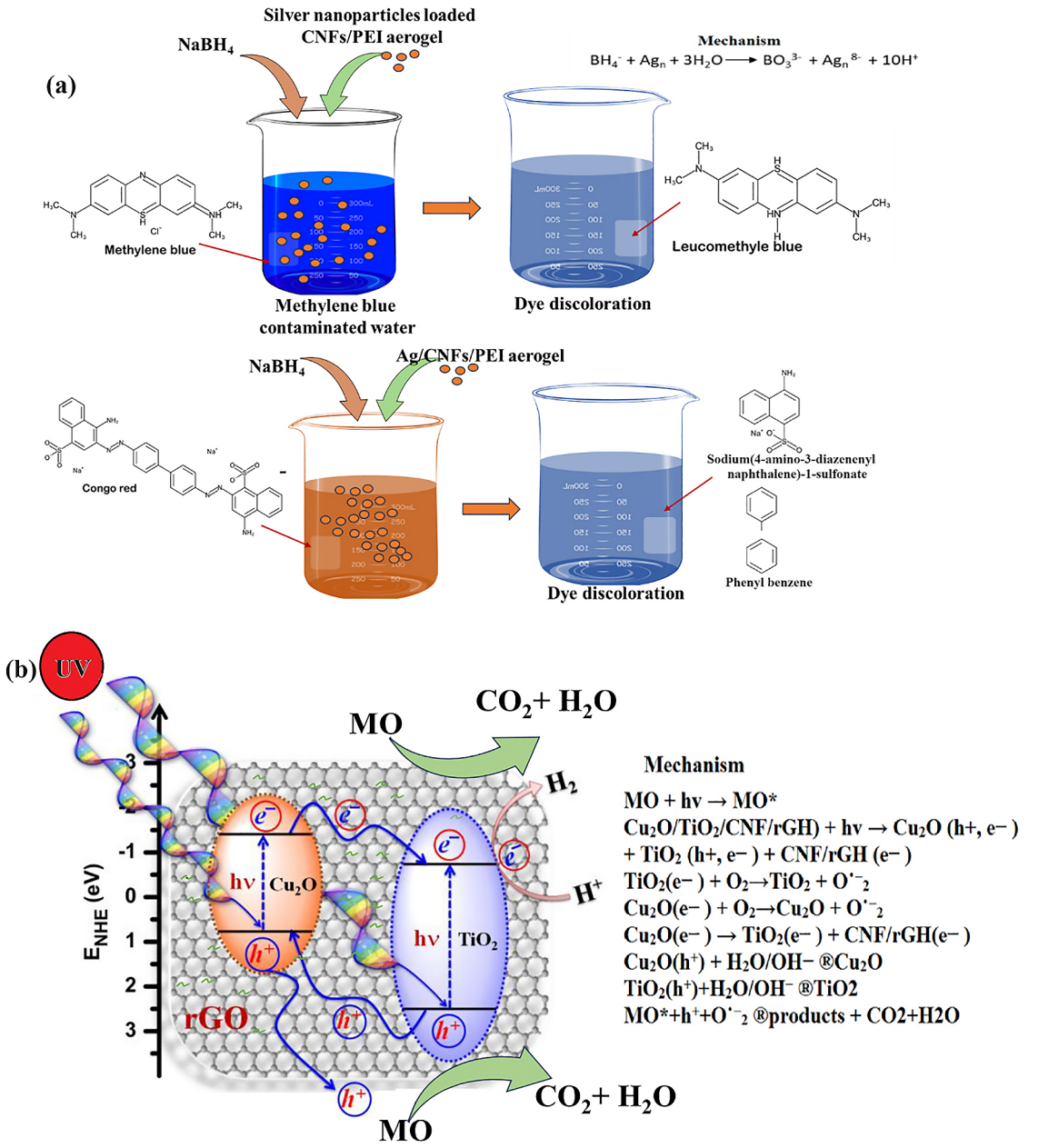

Figure 8. Degradation of dyes using (a) Ag loaded CNFs/PEI [Adopted from Ref. (Raj *et al.*, 2020; Zheng *et al.*, 2022)] and (b) Cu_2O/TiO_2 photo-nano-catalyst loaded CNF/r-GO hydrogels [Adopted from Ref. (Babu *et al.*, 2015; Zheng *et al.*, 2022); A part of figure has been reprinted from Ref. (Babu *et al.*, 2015), Copyright 2015, RSC].

Huang *et al.* (X. Huang *et al.*, 2023) have used this model along with the pseudo-first/second model to study the dye diffusion process on partially fibrillated cationic cellulose adsorbent and found that adsorption follows pseudo-second-order kinetic, confirming the chemisorption (depend upon both adsorbate and adsorbent concentration). Further, through the intraparticle diffusion model, they affirmed that intraparticle diffusion was not the rate-determining step, and the CR adsorption took place through multiple adsorption mechanisms. A couple of other researchers have also used an intraparticle diffusion model while studying adsorption (Beh *et al.*, 2020; X. Huang *et al.*, 2023; T. Zhang *et al.*, 2022). Jamwal *et al.* (Jamwal *et al.*, 2023) used the Elovich equation, which is mostly used for the

confirmation of chemical bonding, in addition to the pseudo-first and second-order model to study the adsorbance of MG dyes onto spherical NC-g-poly (AMPSA) hydrogel and confirmed that adsorbance takes place through pseudo-second order kinetics i.e., through chemisorption pathway. However, no fitting of experimental data to Elovich equation has been affirmed by them. From Table 2, it can be observed that almost all the NC-based aerogels against different dyes follow pseudo-second-order kinetics. However, poly(DMAEMA)/ AMP-ES-CNCs and poly(DMAEMA)/ HMTS-CNCs against MO (Safavi-Mirmahalleh *et al.*, 2020) and Nanobentonite / NC/CS aerogel (V. Sharma *et al.*, 2020) against BB dye have been noticed to obey first-order kinetics, means in these adsorbents the adsorption take place through physical adsorption pathway. Further, in case of TO-CNFs/partially deacetylated chitin hydrogels, the adsorption of MB was noted to follow by both pseudo-first order and pseudo-second order kinetics(X. Zhang *et al.*, 2019) (Fig. 9). In this case, adsorption was noted to increase rapidly for the initial 3 hr and reached adsorption maximum within 12 hr.

Sr. No.	Kinetic Model	Model Equation	Ref.
1	Pseudo First Order	$q_t = q_e (1 - e^{(-k_1 t)})$	(Lagergren, 1898)
2	Pseudo Second Order	$q_t = \frac{k_2 q_e^2 t}{1 + k_2 q_e t}$	(Cheung *et al.*, 2001)
3	Intra Particle Diffusion	$q_t = k_{id} \sqrt{t} + c$	(Weber & Morris, 1963)

Table 3. Adsorption kinetics models

Note: q_e and q_t are the amount of dye adsorbed per unit mass of adsorbent (mg/g) at equilibrium and at time t, respectively; k_1, k_2 and k_{id} is the pseudo-first order sorption rate constant (h^{-1}), pseudo-second order adsorption rate constant (g mg^{-1} h^{-1}) and rate constant of intraparticle diffusion (mg g^{-1} $h^{-0.5}$), respectively and 'c' indicates the thickness of boundary layer.

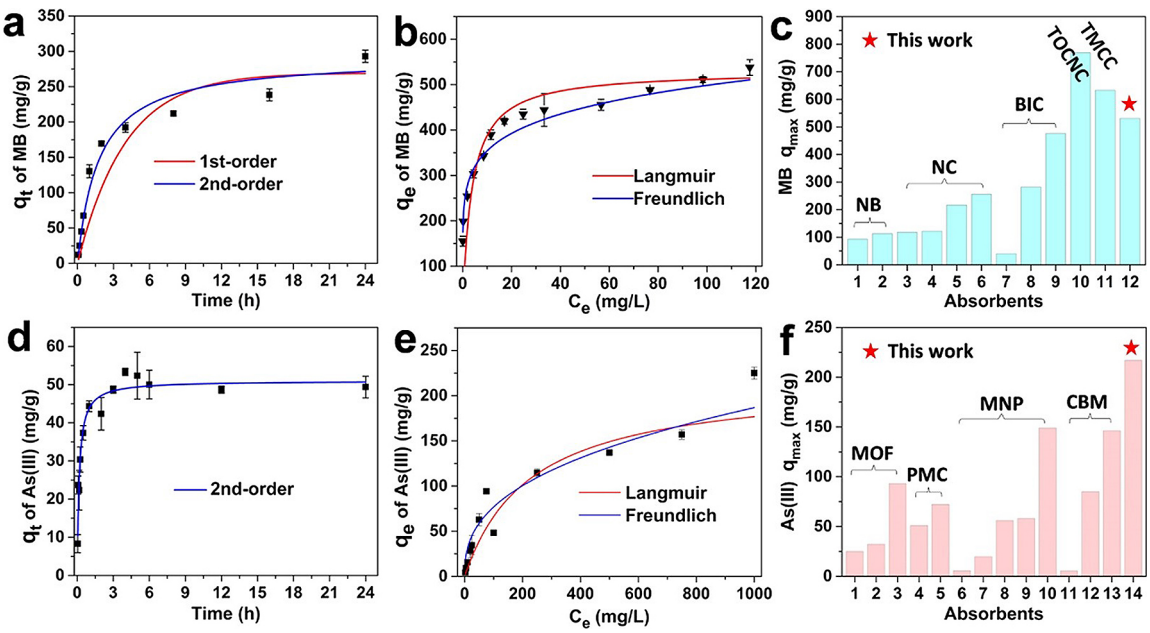

Figure 9. Kinetic models (a) and isothermal models (b) for MB adsorption (pH = 10, C_0 = 50 mg/L, T = 25 °C, t = 24 hr) (X. Zhang *et al.*, 2019). "Reprinted with permission from Ref. (X. Zhang *et al.*, 2019) Copyright 2019, ACS)".

 https://doi.org/10.37819/nanofab.8.1757

7.2. Adsorption isotherm

Several isothermal models, including Langmuir, Freundlich, Temkin, Sips, and Dubinin-Radushkevich, have been used to explore dye adsorption using NC hydrogels as an adsorbent system (Table 4). These models provide useful information about the adsorbent's surface characteristics, the adsorption mechanism, the extent to which adsorption sites are covered, and the degree of affinity between the adsorbent and adsorbate molecules (Al-Ghouti & Da'ana, 2020; Kalam *et al.*, 2021). Table 2 gives the isothermal results of various NC-based adsorbent systems against different dyes. Sometimes, the effects of time and temperature on the rate of adsorption are also taken into account. The information required to find out the adsorption isotherm is generally derived by conducting the static adsorption (batch mode). The concentration of adsorbate is varied to achieve equilibrium adsorption. The equilibrium dye concentration is then plotted against the equilibrium dye uptake and fitted with the aforementioned models. It is crucial to specify the appropriate isotherm model when designing the system and modeling the process since it validates the adsorption process associated with the studied adsorbate-adsorbent system (Kalam *et al.*, 2021).

If the Langmuir isothermal model is determined to be the best fit with the adsorption data, then it validates the homogeneity of the adsorption surface and the monolayer adsorption on an adsorbent surface with a constrained number of uniformly energetic adsorption sites. However, when the Freundlich isotherm model is found to be best fitted, then it confirms multilayer adsorption on heterogeneous adsorbing medium.

Further, to foresee adsorption in heterogeneous systems and get beyond the Freundlich isotherm's restriction on growing adsorbate concentration, the Sips isotherm, which is the combined form of the Langmuir and Freundlich models, might be a good option. This model transforms from Freundlich isotherms to Langmuir isotherms with the increase in adsorbate concentration and may be quite useful for discussing adsorption at a specific pressure or a wide range of pressures (Al-Ghouti & Da'ana, 2020; Tzabar & Ter Brake, 2016). The Temkin model is applicable at the intermediate adsorbate concentration. It presumes multilayer adsorption and studies the adsorbate-adsorbent interactions. Some authors have mentioned that this model is not best-suitable for aqueous adsorption systems, but has still been applied by a couple of researchers to study NC-based dye adsorbing systems. Dubinin-Radushkevich isotherm is also applicable at the intermediate adsorbate concentration and, unlike Langmuir and Freundlich isotherms, this is a semi-empirical equation describing the mechanism of pore filling and is applied to the multilayer physical adsorption process (Al-Ghouti & Da'ana, 2020).

From the table, it can be observed that almost all the NC-based hydrogels have obeyed Langmuir adsorption isotherm against various dyes. However, only three samples i.e., MOF-199@Carboxylated CNC/CMCS (Jiang *et al.*, 2022) (against MB dye), cationic partially fibrillated cellulose (anionic and cationic dyes) (X. Huang *et al.*, 2023) and CNC-CS hydrogels (against CV and MB dyes) (Poornachandhra *et al.*, 2023) have followed Freundlich adsorption isotherm and thus confirmed multilayers adsorption on heterogenous adsorbing medium. Some hydrogels like dialdehyde-CNC/PVAm hydrogel (against CR, AR and reactive light yellow dyes) (Jin *et al.*, 2015), Nanobentonite / NC/CS aerogel (DB and BB) and CNF/MMT/PEI hydrogel (against MB) found to be best fitted to Sips model.

Here, 'q_e', 'C_e', 'Q_o' and 'K_L' are the equilibrium adsorption capacity (mg/g), equilibrium concentration of adsorbate (mg/L), the maximum amount of the dyes adsorbed per unit weight of the adsorbent, mg/g and Langmuir adsorption equilibrium constant, respectively; 'K_F' and 'n' are Freundlich isotherm constant (mg/g) and heterogeneity factor, respectively; 'q_s', 'K_{ad}' and 'ε' are theoretical isotherm saturation capacity (mg/g), Dubinin-Radushkevich isotherm constant (mol^2/kJ^2) and Dubinin-Radushkevich isotherm constant, respectively; 'A_T' 'b_T' and 'R' are Temkin isotherm equilibrium binding constant (L/g), Temkin isotherm constant and universal gas constant (8.314J/mol/K), respectively; and 'bs' is the Sips isotherm constant related to the energy of adsorption.

8. IMPACT OF DIFFERENT FACTORS

The temp, pH, additives and time are major factors that impact significantly the overall performance of the adsorbents and thus special attention has been paid to thoroughly studying the variation in adsorption ability of NC hydrogels with variation in these parameters.

Sr. No.	Name	Model	Linear form	Ref.
1	Langmuir	$q_e = \frac{Q_o K_L C_e}{1 + K_L C_e}$	$q_e = \frac{1}{Q_o} + \frac{K_L C_e}{1 + K_L Q_o C_e}$ $\frac{C_e}{q_e} = \frac{1}{K_L Q_o} + \frac{C_e}{Q_o}$ $q_e = Q_o - \frac{q_e}{K_L C_e}$ $\frac{q_e}{ce} = K_L Q_o - K_L C_e$	(Langmuir, 1918)
2	Freundlich	$q_e = K_F C_e^{1/n}$	$\log qe = \log K_F + \frac{1}{n} \log C_e$	(Piccin *et al.*, 2011)
3	Dubinin-Radushkevich	$q_e = (q_s)\exp(-K_{ad}\varepsilon^2)$	$\ln(qe) = \ln(qs) - (K_{ad}\varepsilon^2)$	(Dubinin, 1960)
4	Temkin	$q_e = \frac{RT}{b_T} \ln(A_t C_e)$	$q_e = \frac{RT}{b_T} \ln A_T C_e + (\frac{RT}{b_T}) \ln C_e$	(Temkin, 1940)
5	Sips	$q_e = \frac{q_m b_s C_e^{\frac{1}{n}}}{1 + b_s C_e^{\frac{1}{n}}}$	$\ln\left(\frac{q_e}{q_m - q_e}\right) = \frac{1}{n} \ln(b_s) + \ln(b_s)^{\frac{1}{n}}$	(Sips, 1948)

Table 4. Different isotherm models used for the adsorption of dyes.

8.1. Impact of additives or functionalization

Efforts have been made to enhance the adsorbing nature or functionality of NC-based hydrogel by blending it with various bio-nanofillers of different functionalities or oxidized/functionalized with suitable polymers. The addition of additives/functional groups not only enhances the surface chemistry but also helps in controlling the pore size, surface area, density, etc., of the hydrogel. The addition of fillers can be carried out with or without cross-linkers. Yap *et al.* (Yap *et al.*, 2023) blended SA /CMC with NC and reported an increase in adsorption tendency from 24.4 to 90.1% towards MB. Roa *et al.* (Roa *et al.*, 2021) graft copolymerized CNFs with ALETA monomer utilizing MBA cross-linkers through a free radical reaction pathway for enhancing CNFs tendency to adsorb MY dye. Xu *et al.* (Xue *et al.*, 2023) found that with the increase in carboxyl groups amount in TO-CNFs hydrogels, the rate of MB dye adsorption increases and attains equilibrium at 50 min. Further, they reported an increase in adsorption capacity from 538 to 682 mg/g, when the concentration of hypochlorite, treatment applied to obtain the TO-CNFs with different carboxyl contents, was varied from 2.5 to 10 mmol /L. Such an increased adsorption capability because of enhancement in porous structure, pore numbers and specific surface area of hydrogel with an increase in carboxylate contents has been reported by a couple of researchers (Mishnaevsky *et al.*, 2019; Xue *et al.*, 2023). Di-aldehyde CNCs were reacted with PVAm to introduce the new functional groups (NH_2 and COOH groups) on CNCs surface, which ultimately enhanced CNCs adsorbing capability towards AR, CR 4BS and reactive light yellow K-4G dyes (Jin *et al.*, 2015). Similarly, a lot of polymers like AA-co-HEMA (Hosseinzadeh *et al.*, 2019), poly(AMPSA) (Jamwal *et al.*, 2023) and Girad,s reagent(X. Huang *et al.*, 2023) have been introduced on CNCs, spherical NC and partially nanofibrilled cellulose, respectively, to enhance the adsorption capability of virgin NC.

MOFs like MOF-199 (Jiang *et al.*, 2022), montmorillonite (R. Huang *et al.*, 2023; X. Zhang *et al.*, 2023) and UIO-66 (Z. Wang *et al.*, 2019), due to their high crystallinity, porous nature, tailor able pore size and surface characteristics, alluring absorption ability and high specific surface area, have also been added as fillers in NC hydrogels to enhance their dye adsorbing capability. *Zhangu et al.* (Jiang *et al.*, 2022) prepared MOF-199@Carboxylated CNC/CMCS hybrid through the coordination bonding and ionic cross-linking between MOF-199, and CMCS and carboxylated CNC. The developed aerogel showed a recordable adsorption ability of 1112.2 mg/g against MB, which is the best among entire NC-based hydrogels developed for MB dye adsorption. Further, GO, because of the presence of numerous oxygen-containing groups like -OH, -COOH and epoxy groups and higher surface area have also been utilized as fillers to enhance the porosity, mechanical strength and adsorption ability of NC hydrogels (Al-Shemy *et al.*, 2022; Nguyen *et al.*, 2022; Shandong Agricultural University *et al.*, 2019; Z. Wang *et al.*, 2021) (Table 2). Among different samples, the CNFs/GO hydrogel prepared by Zhang *et al.* (Z. Wang *et al.*, 2021) without any use of cross-linkers showed maximum adsorption of 111.2 mg/g against MB within 6 min, which is the highest among all GO-based samples in minimum time. The CNFs/GO composite hydrogels synthesized by Wei *et al.* (Shandong Agricultural University *et al.*, 2019) showed maximum percent adsorption, among all samples, against MB; however, the time taken is quite long (24 hr). Natural polysaccharides like CS (Jiang *et al.*, 2022; Poornachandhra *et al.*, 2023) and SA (Al-Shemy *et al.*, 2022) owing to the presence of $-NH_2$ and -OH, and -COOH and -OH groups, respectively, have also been used as fillers for enhancing the pore size as well as functionality for better dye adsorption.

Nowadays, metal/metal oxide photocatalysts, due to their eco-friendly nature and advantageous optical characteristics, have been frequently utilized for the degradation of dyes (Ahmaruzzaman & Mishra, 2021; H. Kumari *et al.*, 2023). However, there are a few things that are limiting their use as photocatalysts in water purification. These include the agglomeration of nanoparticles because of high surface area/energy during the treatment and removal issues. There have been considerable attempts made to address this issue by using NC-based 3D support aerogel to decorate/support photo nanocatalysts, which will not only resolve the agglomeration issue but also make it simple to remove the nanocatalyst after -treatment (Ferreira-Neto *et al.*, 2020; W. Zhang *et al.*, 2020; Zheng *et al.*, 2022). Zhang *et al.* (W. Zhang *et al.*, 2020) loaded Ag nanoparticles onto CNFs/PEI hydrogels, Zheng *et al.* (Zheng *et al.*, 2022) decorated Cu_2O/TiO_2 onto CNFs/r-GO hydrogels and Ferreira-Neto *et al.* (Ferreira-Neto *et al.*, 2020) loaded MoS_2 photocatalytic nanoparticles onto BC hydrogels for effective removal of dyes. Due to the synergistic impact of photo nanocatalyst-loaded aerogel as an adsorbent and as a dye degrader, these materials showed the remarkable capability to remove dyes from wastewater. Zhang *et al.* (W. Zhang *et al.*, 2020) recorded a dye degradation of 99.2% for MB (within 5 min) and 96.4% for CR (21 min), when they employed CNFs/PEI/Ag aerogels along with $NaBH_4$ as a reducing agent. Zheng *et al.* (Zheng *et al.*, 2022) reported 85.62% MO dye degradation capability for Cu_2O/TiO_2/CNF/r-GO, when irradiated with UV light for 120 min. Similarly, a degradation of 96±3% was noted for MB dye, on utilization of BC/MoS_2 adsorbents and irradiating the dye solution for 120 min with UV-visible light (Ferreira-Neto *et al.*, 2020).

8.2. Effect of pH

The point of zero charge (pHpzc) value of the adsorbent controls its ability to adsorb anionic and cationic dyes (Ibrahim *et al.*, 2010). Adsorption of cationic dyes is favored when the solution pH value lies > pHpzc of the adsorbent and similarly, anionic dyes adsorbance is expected to be favored when the solution pH lies < pHpzc of the adsorbent. A lot of work has been done in studying the impact of pH on dye adsorbing capability of NC-based hydrogels against different cationic (MB, MG, rhodamine B, BBY, BCB, CV, etc.) and anionic dyes (MO, CR, AG25, ARS, ABM, BB, DB, etc.). Jin *et al.* (Jin *et al.*, 2015) while studying the adsorbing capability of dialdehyde-CNC/PVAm (pHpzc value 5.6) hydrogel against CR dyes, reported an increase in removal efficiency (from 59.9 to 99.9%) with the decrease in pH of solution (from 9 to 3.5, respectively). This increase in adsorption has been attributed to the protonation of amine group (NH_3^+), available on hydrogel surface, in an acidic medium causing enhanced electrostatic interaction between NH_3^+ group of hydrogel and SO_3^{2-} groups of CR dye. On further enhancing the pH of a solution, the deprotonation NH_3^+ group occurs, which in turn lowers the electrostatic interaction with anionic

dye and thus lowers adsorption. Pooranchandra *et al.* (Poornachandhra *et al.*, 2023) reported a 4.4 pHpzc value for CNC-CS hydrogels, meaning the surface of this hydrogel remains neutral at this pH. However, when pH was increased beyond 4.4 (from 5 to 9) the adsorbent surface became -ve charged because of deprotonation of carboxyl (-COO) and amino (-NH_2) groups available on the adsorbent surface and thus its tendency to adsorb MB cationic dye enhanced from 86 to 90%. Similarly, Xue *et al.* (Xue *et al.*, 2023), when utilizing TO-CNFs hydrogel adsorbents for MB adsorption, also reported an increase in removal capacity from 395 to 682 mg/g with enhancement in pH from 3 to 9. Zhang *et al.* (Z. Zhang, Hu, *et al.*, 2022) found maximum adsorption at pH 5.25 for MOF-199@Carboxylated CNC/CMCS aerogel against MB, which is higher than the pHpzc value (4.3) reported for same adsorbing hydrogel by Mullet *et al.* (Mullet *et al.*, 1999). A strong decrease in MB adsorption from 100 to 10% was found for sago pitch waste extracted CNFs hydrogel upon the decrease in pH from 7 to 5 (Beh *et al.*, 2020). Similarly, Zhang *et al.* also better adsorption ability of CNF/MMT/PEI hydrogel towards MB at a pH higher than pHpzc value of hydrogel (Fig. 10) (X. Zhang *et al.*, 2023). Jamwal *et al.* (93) found a sharp increase in MG adsorption ability for NC-g-poly(AMPSA) hydrogels when pH was increased beyond pHpzc value of hydrogel. Ruan *et al.* (Ruan *et al.*, 2022) found an increase in the adsorption of MB dye on CNCs/SiO_2 hydrogels upon an increase in pH from 2 to 10. A sharp increase (218.3 to 265.9 mg/g) in adsorption was reported for PDA-CNFs-PEI hydrogels against MO dye when pH was decreased from 10.2 to 4.41 (Tang *et al.*, 2019). This has been attributed to protonation of PEI resulting in enhanced electrostatic attraction with anionic MO dye.

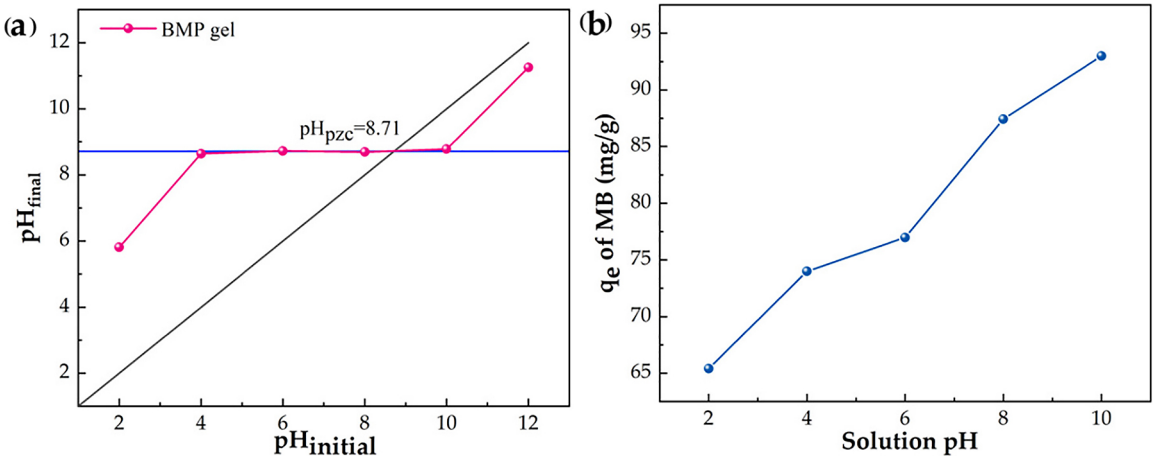

Figure 10. (a) pHpzc of CNF/MMT/PEI hydrogel hydrogels and (b) Variation in adsorption of MB dye on CNF/MMT/PEI hydrogel hydrogels with pH (X. Zhang *et al.*, 2023) "Reprinted from Ref. (X. Zhang *et al.*, 2023), MDPI, under CC BY 4.0)".

8.3. Impact of temperature

Some authors have reported an increase in dye adsorption ability of NC-based adsorbents with an increase in temperature, while others have reported the opposite trend. For example, Hosseinzadeh *et al.* (Hosseinzadeh *et al.*, 2019) found that when the temperature is increased from 25 to 55°C, the rate of diffusion of CV dye on CNCs-g-poly(AA-co-HEMA) increases, suggesting the adsorption process is endothermic. Zhang and coworkers also reported an increase in adsorption of MB onto CNF/ MMT/PEI hydrogel with the increase in temperature from 25 to 45°C (X. Zhang *et al.*, 2023). A couple of research groups, Xue *et al.* (Xue *et al.*, 2023) and Al-Shemy *et al.* (Al-Shemy *et al.*, 2022) also demonstrated the adsorption process to be endothermic during their study on adsorption of MB onto TO-CNFS and SA/GO/CNC 3d scaffold, respectively. Jamwal *et al.* (Jamwal *et al.*, 2023) contrary to the above finding, demonstrated a rise in adsorption of MG dye onto NC-g-poly (AMPSA) hydrogel up to 30°C, but beyond that a small decrease in adsorption was noted by them. Tavakolian *et al.* (Tavakolian *et al.*, 2020) also reported a 10% decrease in MB dye adsorption for SA-electrostatically stabilized CNCs adsorbents, when the temperature was increased from 20 to 60°C, suggesting that adsorption is exothermic reaction.

9. REGENERATION OR RECYCLING

The reusability and regenerability study of adsorbents is of importance as it will make the adsorption process of dye removal economical. The majority of researchers have used hydrochloric acid as an eluent for the regeneration of NC-based hydrogels (Roa *et al.*, 2021; Xue *et al.*, 2023). Roa *et al.* (Roa *et al.*, 2021) recommended that poly(AETAC]-g- 1 % TO-CNF hydrogels can be recycled three times, because of a sudden fall in their adsorption capability after the third cycle. Xue *et al.* (Xue *et al.*, 2023) have utilized four different eluents, namely deionized water, ethanol, NaOH solution (1 mol/L), and HCl solution (1 mol /L) to study the desorption of MB from TO-CNFs beads. The maximum desorption was found with ethanol (94%) followed by HCl solution (93%), water (45%) and NaOH solution (34%). Further, when HCl solution was utilized multiple times, the hydrogels showed 83% MB removal efficiency even after the fifth cycle. Hosseinzadeh *et al.* (Hosseinzadeh *et al.*, 2019) carried out adsorption-desorption cycle of P(AA-co-HEMA)-g-CNC against CV dye in both acidic (pH:3) and basic medium (pH:9). They reported better dye adsorption capability for hydrogels in the basic medium (71 mg/g) than in acidic medium (11%) after the fifth regeneration cycle. Poornachandhra *et al.* (Poornachandhra *et al.*, 2023) while studying the desorption of CV and MB dyes from CNC-CS hydrogels, found that the eluents like NaOH (1M) and KOH (1 M) perform well in the case of CV desorption, while 50% ethanol and HCl (0.1 M) solution give best results against MB dye. GO-based NC hydrogels also showed promising results while recycling multiple times by simply washing with ethanol. CNFs/GO demonstrated removal efficiency of 98% against MB and 97% against TC after the 3rd cycle (Z. Wang *et al.*, 2021). Similarly, another group reported 91.1% removal efficiency for CNFs/GO against MB after 5th cycle (Nguyen *et al.*, 2022) (Fig. 11). Jamwal *et al.* (93) during reusability of NC-g-poly(AMPSA) hydrogels, varied the concentration of eluents (HCl acid) from 0.10 N -0.75 N. They reported maximum RE or q_m at 0.50 N HCl concentration after the 8th cycle. Li *et al.* (Q. Li *et al.*, 2021) used 2% NaOH solution for desorption of MO from CNC-PEI-beta-cyclodextrin/poly(AAm) hydrogel and they reported a remarkable removal efficiency of 76.67% after the fifth cycle. From table 2, we can notice that metal or metal oxide-based hydrogels, even after the 7-8th catalytic process, give better/highest dye discoloration ability. For example, CNFs/ PEI/Ag showed a dye discoloration tendency of 98% (against MB and CR) (W. Zhang *et al.*, 2020), Cu_2O/TiO_2/CNF/reduced graphene hydrogel showed 79.5% against MO (Zheng *et al.*, 2022) and Bacterial NC/MoS_2 hybrid hydrogels showed 86% against MB, after the 10th , 4th and 6th catalytic process, respectively (Ferreira-Neto *et al.*, 2020).

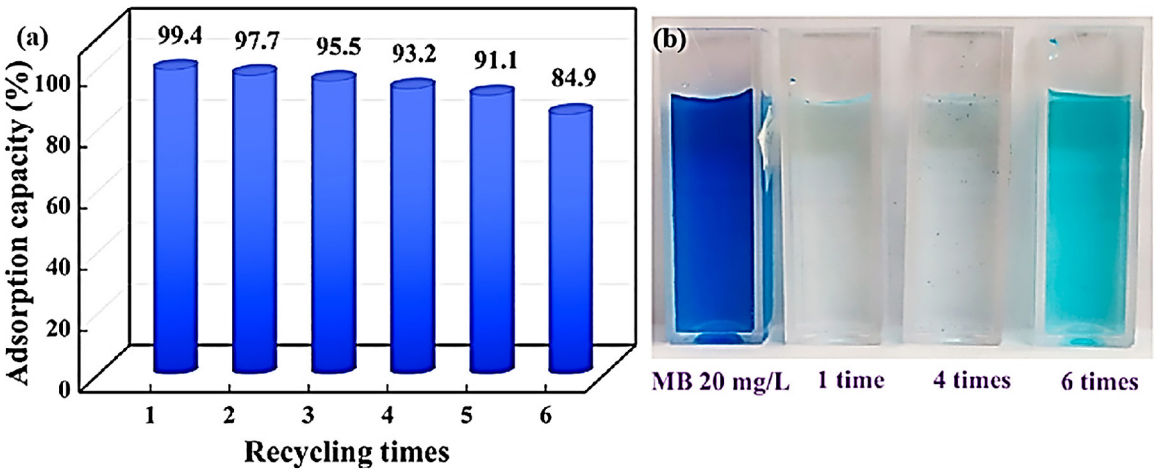

Figure 11. (a) Variation in MB adsorption capacity of CNFs/GO hydrogel after recycling and (b) changes in the color of MB solutions after 1, 4, and 6 recycles (Nguyen *et al.,* 2022). "Reprinted from ref. (Nguyen *et al.,* 2022), Copyright 2022, ACS, under CC BY 4.0)".

10. CONCLUSION

This review provides a brief overview of the removal of dyes using NC hydrogel-based adsorbents. These adsorbents, in addition to their sustainable, cost-effective and eco-friendly nature, also displayed a phenomenal rate of adsorption. It has been established that blending or functionalizing NC hydrogels directly contributes to the improvement of their adsorption ability. So far various cross-linkers have been applied to crosslink the NC-based hydrogels and have resulted in enhancement in the NC hydrogels' dye adsorption ability. Further, the different nanofillers/blenders used were MOFs, Ag metals, Cu_2O, SiO_2, CS, etc. The metals/metal oxide-filled NC-hydrogels, due to the synergistic effect of adsorption and photocatalytic degradation showed huge potential in dye removal. Among different samples, the dialdehyde-CNC/ PVAm hydrogel and MOF-199@Carboxylated CNC/CMCS hydrogels had the best dye adsorption potential. The factors like initial dye concentration, solution pH, adsorbent dosage, temperature and time impact significantly the ability of NC hydrogel-based adsorbents to remove dye from wastewater. Furthermore, through kinetics research, it has been affirmed the majority of adsorption occurs via a pseudo-second-order reaction. Hydrogels have been recycled by treating them with alkali, ethanol, acid and water. The recycled hydrogels showed an alluring capability to adsorb the dyes even after the 5-8th cycle. Thus, we can conclude that NC hydrogel-based adsorbents are extremely efficient for the treatment of wastewater and are also renewable and reusable.

However, there is still a need to undergo significant technological advancements before they can be implemented in practical applications. The following is a list of the challenges and upcoming angles to the present study problem. Large-scale development of NC hydrogels is very challenging; efforts are still needed to optimize the number of additives based on the porosity and adsorption capacity of the hydrogels; bio-degradation may be a problem as crosslinkers may inhibit their ability to degrade; the cost of NC extraction is high; and actions are still needed to assess the life cycle of NC hydrogels. ♦

REFERENCES

Aegerter, M. A., Leventis, N., & Koebel, M. A. (Eds.). (2011). *Aerogels handbook*. Springer.

Ahmad, A., Kamaruddin, M. A., H.P.S., A. K., Yahya, E. B., Muhammad, S., Rizal, S., Ahmad, M. I., Surya, I., & Abdullah, C. K. (2023). Recent Advances in Nanocellulose Aerogels for Efficient Heavy Metal and Dye Removal. *Gels*, *9*(5), 416. https://doi.org/10.3390/gels9050416

Ahmaruzzaman, Md., & Mishra, S. R. (2021). Photocatalytic performance of g-C3N4 based nanocomposites for effective degradation/removal of dyes from water and wastewater. *Materials Research Bulletin*, *143*, 111417. https://doi.org/10.1016/j.materresbull.2021.111417

Akhtar, M. F., Hanif, M., & Ranjha, N. M. (2016). Methods of synthesis of hydrogels … A review. *Saudi Pharmaceutical Journal*, *24*(5), 554-559. https://doi.org/10.1016/j.jsps.2015.03.022

Akter, M., Bhattacharjee, M., Dhar, A. K., Rahman, F. B. A., Haque, S., Rashid, T. U., & Kabir, S. M. F. (2021). Cellulose-Based Hydrogels for Wastewater Treatment: A Concise Review. *Gels*, *7*(1), 30. https://doi.org/10.3390/gels7010030

Al-Ghouti, M. A., & Da'ana, D. A. (2020). Guidelines for the use and interpretation of adsorption isotherm models: A review. *Journal of Hazardous Materials*, *393*, 122383. https://doi.org/10.1016/j.jhazmat.2020.122383

Al-Sabah, A., Burnell, S. E., Simoes, I. N., Jessop, Z., Badiei, N., Blain, E., & Whitaker, I. S. (2019). Structural and mechanical characterization of crosslinked and sterilised nanocellulose-based hydrogels for cartilage tissue engineering. *Carbohydrate Polymers*, *212*, 242-251.

Al-Shemy, M. T., Al-Sayed, A., & Dacrory, S. (2022). Fabrication of sodium alginate/graphene oxide/nanocrystalline cellulose scaffold for methylene blue adsorption: Kinetics and thermodynamics study. *Separation and Purification Technology*, *290*, 120825. https://doi.org/10.1016/j.seppur.2022.120825

Amor, C., Marchão, L., Lucas, M. S., & Peres, J. A. (2019). Application of advanced oxidation processes for the treatment of recalcitrant agro-industrial wastewater: A review. *Water*, *11*(2), 205.

Babu, S. G., Vinoth, R., Praveen Kumar, D., Shankar, M. V., Chou, H.-L., Vinodgopal, K., & Neppolian, B. (2015). Influence of electron storing, transferring and shuttling assets of reduced graphene oxide at the interfacial copper doped TiO_2 p-n heterojunction for increased hydrogen production. *Nanoscale*, *7*(17), 7849-7857. https://doi.org/10.1039/C5NR00504C

Barbucci, R., Consumi, M., Lamponi, S., & Leone, G. (2003). Polysaccharides based hydrogels for biological applications. *Macromolecular Symposia, 204*(1), 37-58.

Beh, J. H., Lim, T. H., Lew, J. H., & Lai, J. C. (2020). Cellulose nanofibril-based aerogel derived from sago pith waste and its application on methylene blue removal. International *Journal of Biological Macromolecules, 160*, 836-845. https://doi.org/10.1016/j.ijbiomac.2020.05.227

Berglund, L., Squinca, P., Baş, Y., Zattarin, E., Aili, D., Rakar, J., Junker, J., Starkenberg, A., Diamanti, M., Sivlér, P., Skog, M., & Oksman, K. (2023). Self-Assembly of Nanocellulose Hydrogels Mimicking Bacterial Cellulose for Wound Dressing Applications. *Biomacromolecules, 24*(5), 2264-2277. https://doi.org/10.1021/acs.biomac.3c00152

Bhaladhare, S., & Das, D. (2022). Cellulose: A fascinating biopolymer for hydrogel synthesis. *Journal of Materials Chemistry B, 10*(12), 1923-1945. https://doi.org/10.1039/D1TB02848K

Bhatnagar, A., Sillanpää, M., & Witek-Krowiak, A. (2015). Agricultural waste peels as versatile biomass for water purification – A review. *Chemical Engineering Journal, 270*, 244-271. https://doi.org/10.1016/j.cej.2015.01.135

Bokov, D., Turki Jalil, A., Chupradit, S., Suksatan, W., Javed Ansari, M., Shewael, I. H., Valiev, G. H., & Kianfar, E. (2021). Nanomaterial by Sol-Gel Method: Synthesis and Application. *Advances in Materials Science and Engineering, 2021*, 1-21. https://doi.org/10.1155/2021/5102014

Cai, J., Zhang, D., Xu, W., Ding, W.-P., Zhu, Z.-Z., He, J.-R., & Cheng, S.-Y. (2020). Polysaccharide-based hydrogels derived from cellulose: The architecture change from nanofibers to hydrogels for a putative dual function in dye wastewater treatment. *Journal of Agricultural and Food Chemistry, 68*(36), 9725-9732.

Chau, M., De France, K. J., Kopera, B., Machado, V. R., Rosenfeldt, S., Reyes, L., Chan, K. J. W., Förster, S., Cranston, E. D., Hoare, T., & Kumacheva, E. (2016). Composite Hydrogels with Tunable Anisotropic Morphologies and Mechanical Properties. *Chemistry of Materials, 28*(10), 3406-3415. https://doi.org/10.1021/acs.chemmater.6b00792

Chaudhary, J., Thakur, S., Mamba, G., Prateek, Gupta, R. K., & Thakur, V. K. (2021). Hydrogel of gelatin in the presence of graphite for the adsorption of dye: Towards the concept for water purification. *Journal of Environmental Chemical Engineering, 9*(1), 104762. https://doi.org/10.1016/j.jece.2020.104762

Chen, C., Xi, Y., & Weng, Y. (2022). Recent advances in cellulose-based hydrogels for tissue engineering applications. *Polymers, 14*(16), 3335.

Cheung, C. W., Porter, J. F., & Mckay, G. (2001). Sorption kinetic analysis for the removal of cadmium ions from effluents using bone char. *Water Research, 35*(3), 605-612. https://doi.org/10.1016/S0043-1354(00)00306-7

Ching, T. W., Haritos, V., & Tanksale, A. (2018). Ultrasound-assisted conversion of cellulose into hydrogel and functional carbon material. *Cellulose, 25*(4), 2629-2645. https://doi.org/10.1007/s10570-018-1746-y

Chu, K. H., Mang, J. S., Lim, J., Hong, S., & Hwang, M.-H. (2021). Variation of free volume and thickness by high pressure applied on thin film composite reverse osmosis membrane. *Desalination, 520*, 115365.

Costa, F. C., dos Santos, C. R., & Amaral, M. C. (2023). Trace organic contaminants removal by membrane distillation: A review on mechanisms, performance, applications, and challenges. *Chemical Engineering Journal, 464*, 142461.

Dąbrowski, A. (2001). Adsorption—From theory to practice. *Advances in Colloid and Interface Science, 93*(1-3), 135-224. https://doi.org/10.1016/S0001-8686(00)00082-8

Dai, L., Cheng, T., Wang, Y., Lu, H., Nie, S., He, H., Duan, C., & Ni, Y. (2019). Injectable all-polysaccharide self-assembling hydrogel: A promising scaffold for localized therapeutic proteins. *Cellulose, 26*, 6891-6901.

De France, K. J., Hoare, T., & Cranston, E. D. (2017). Review of Hydrogels and Aerogels Containing Nanocellulose. *Chemistry of Materials, 29*(11), 4609-4631. https://doi.org/10.1021/acs.chemmater.7b00531

Dubinin, M. M. (1960). The Potential Theory of Adsorption of Gases and Vapors for Adsorbents with Energetically Nonuniform Surfaces. *Chemical Reviews, 60*(2), 235-241. https://doi.org/10.1021/cr60204a006

El Bouazzaoui, Y., Habsaoui, A., & Touhami, M. E. (2022). Hydrogel synthesis using extracted cellulose from Opuntia Ficus indica seeds and its application in methylene blue dye removal. *Chemical Data Collections, 41*, 100918.

Febrianto, J., Kosasih, A. N., Sunarso, J., Ju, Y.-H., Indraswati, N., & Ismadji, S. (2009).

Equilibrium and kinetic studies in adsorption of heavy metals using biosorbent: A summary of recent studies. *Journal of Hazardous Materials*, *162*(2-3), 616-645. https://doi.org/10.1016/j.jhazmat.2008.06.042

Ferreira-Neto, E. P., Ullah, S., Da Silva, T. C. A., Domeneguetti, R. R., Perissinotto, A. P., De Vicente, F. S., Rodrigues-Filho, U. P., & Ribeiro, S. J. L. (2020). Bacterial Nanocellulose/MoS_2 Hybrid Aerogels as Bifunctional Adsorbent/Photocatalyst Membranes for in-Flow Water Decontamination. *ACS Applied Materials & Interfaces*, *12*(37), 41627-41643. https://doi.org/10.1021/acsami.0c14137

Fotie, G., Rampazzo, R., Ortenzi, M. A., Checchia, S., Fessas, D., & Piergiovanni, L. (2017). The effect of moisture on cellulose nanocrystals intended as a high gas barrier coating on flexible packaging materials. *Polymers*, *9*(9), 415.

Guastaferro, M., Baldino, L., Reverchon, E., & Cardea, S. (2021). Production of Porous Agarose-Based Structures: Freeze-Drying vs. Supercritical CO_2 Drying. *Gels*, *7*(4), 198. https://doi.org/10.3390/gels7040198

Gulrez, S. K. H., Al-Assaf, S., Phillips, G. O., Gulrez, S. K. H., Al-Assaf, S., & Phillips, G. O. (2011). Hydrogels: Methods of Preparation, Characterisation and Applications. In *Progress in Molecular and Environmental Bioengineering – From Analysis and Modeling to Technology Applications*. IntechOpen. https://doi.org/10.5772/24553

Günay, A., Arslankaya, E., & Tosun, İ. (2007). Lead removal from aqueous solution by natural and pretreated clinoptilolite: Adsorption equilibrium and kinetics. *Journal of Hazardous Materials*, *146*(1-2), 362-371. https://doi.org/10.1016/j.jhazmat.2006.12.034

Gurav, J. L., Jung, I.-K., Park, H.-H., Kang, E. S., & Nadargi, D. Y. (2010). Silica Aerogel: Synthesis and Applications. Journal of Nanomaterials, 2010, 1-11. https://doi.org/10.1155/2010/409310

Hammami, C., & René, F. (1997). Determination of freeze-drying process variables for strawberries. *Journal of Food Engineering*, *32*(2), 133-154. https://doi.org/10.1016/S0260-8774(97)00023-X

Hosseinzadeh, S., Hosseinzadeh, H., & Pashaei, S. (2019). Fabrication of nanocellulose loaded poly(AA- co -HEMA) hydrogels for ceftriaxone controlled delivery and crystal violet adsorption. *Polymer Composites*, *40*(S1). https://doi.org/10.1002/pc.24875

Hsu, C.-J., Xiao, Y.-Z., Chung, A., & Hsi, H.-C. (2023). Novel applications of vacuum distillation for heavy metals removal from wastewater, copper nitrate hydroxide recovery, and copper sulfide impregnated activated carbon synthesis for gaseous mercury adsorption. *Science of The Total Environment*, *855*, 158870.

Huang, R., Xu, Y., Kuznetsov, B. N., Sun, M., Zhou, X., Luo, J., & Jiang, K. (2023). Enhanced hybrid hydrogel based on wheat husk lignin-rich nanocellulose for effective dye removal. *Frontiers in Bioengineering and Biotechnology*, *11*, 1160698. https://doi.org/10.3389/fbioe.2023.1160698

Huang, S., Wu, L., Li, T., Xu, D., Lin, X., & Wu, C. (2019). Facile preparation of biomass lignin-based hydroxyethyl cellulose super-absorbent hydrogel for dye pollutant removal. International *Journal of Biological Macromolecules, 137,* 939-947.

Huang, X., Hadi, P., Joshi, R., Alhamzani, A. G., & Hsiao, B. S. (2023). A Comparative Study of Mechanism and Performance of Anionic and Cationic Dialdehyde Nanocelluloses for Dye Adsorption and Separation. *ACS Omega*, *8*(9), 8634-8649. https://doi.org/10.1021/acsomega.2c07839

Ibrahim, S., Fatimah, I., Ang, H.-M., & Wang, S. (2010). Adsorption of anionic dyes in aqueous solution using chemically modified barley straw. *Water Science and Technology*, *62*(5), 1177-1182. https://doi.org/10.2166/wst.2010.388

Jamwal, P., Chauhan, G. S., Kumar, P., Kumari, B., Kumar, K., & Chauhan, S. (2023). A study in the synthesis of new Pinus wallichiana derived spherical nanocellulose hydrogel and its evaluation as malachite green adsorbent. *Sustainable Chemistry and Pharmacy*, *32*, 100950. https://doi.org/10.1016/j.scp.2022.100950

Jawaid, M., & Mohammad, F. (2017). *Nanocellulose and Nanohydrogel Matrices: Biotechnological and Biomedical Applications.* John Wiley & Sons.

Jedrzejczak-Krzepkowska, M., Kubiak, K., Ludwicka, K., & Bielecki, S. (2016). Bacterial nanocellulose synthesis, recent findings. In *Bacterial Nanocellulose* (pp. 19-46). Elsevier.

Jiang, M., Zhang, Z., Hu, J., Tian, X., Guo, F., Wang, C., & Zhang, J. (2022). Facile In-Situ Growth of Mof-199 Layer on Carboxylated Nanocellulose/Chitosan Aerogel Spheres and Their High-Efficient Adsorption and Catalytic Performance. *SSRN Electronic Journal.* https://doi.org/10.2139/ssrn.4080987

Jin, L., Sun, Q., Xu, Q., & Xu, Y. (2015). Adsorptive removal of anionic dyes from aqueous solutions using microgel based on nanocellulose and polyvinylamine. *Bioresource Technology, 197,* 348-355.

Kalam, S., Abu-Khamsin, S. A., Kamal, M. S., & Patil, S. (2021). Surfactant Adsorption Isotherms: A Review. *ACS Omega, 6*(48), 32342-32348. https://doi.org/10.1021/acsomega.1c04661

Kang, H., Liu, R., & Huang, Y. (2016). Cellulose-Based Gels. *Macromolecular Chemistry and Physics, 217*(12), 1322-1334.

Kaushik, J., Gunture, Tripathi, K. M., Singh, R., & Sonkar, S. K. (2022). Thiourea-functionalized graphene aerogel for the aqueous phase sensing of toxic Pb(II) metal ions and H2O2. *Chemosphere, 287,* 132105. https://doi.org/10.1016/j.chemosphere.2021.132105

Kaushik, J., Kumar, V., Garg, A. K., Dubey, P., Tripathi, K. M., & Sonkar, S. K. (2021). Biomass derived functionalized graphene aerogel: A sustainable approach for the removal of multiple organic dyes and their mixtures. *New Journal of Chemistry, 45*(20), 9073-9083. https://doi.org/10.1039/D1NJ00470K

Kaushik, J., Sharma, C., Lamba, N. K., Sharma, P., Das, G. S., Tripathi, K. M., Joshi, R. K., & Sonkar, S. K. (2023). 3D Porous MoS_2 -Decorated Reduced Graphene Oxide Aerogel as a Heterogeneous Catalyst for Reductive Transformation Reactions. *Langmuir, 39*(36), 12865-12877. https://doi.org/10.1021/acs.langmuir.3c01785

Kayra, N., & Aytekin, A. Ö. (2018). Synthesis of Cellulose-Based Hydrogels: Preparation, Formation, Mixture, and Modification. In Md. I. H. Mondal (Ed.), Cellulose-Based Superabsorbent Hydrogels (pp. 1-28). *Springer International Publishing.* https://doi.org/10.1007/978-3-319-76573-0_16-1

Kumari, H., Sonia, Suman, Ranga, R., Chahal, S., Devi, S., Sharma, S., Kumar, S., Kumar, P., Kumar, S., Kumar, A., & Parmar, R. (2023). A Review on Photocatalysis Used For Wastewater Treatment: Dye Degradation. *Water, Air, & Soil Pollution, 234*(6), 349. https://doi.org/10.1007/s11270-023-06359-9

Kumari, P., Disha, Nayak, M. K., Dhruwe, D., Patel, M. K., & Mishra, S. (2023). Synthesis and characterization of sulfonated magnetic graphene-based cation exchangers for the removal of methylene blue from aqueous solutions. *Industrial & Engineering Chemistry Research, 62*(3), 1245-1256.

Lagergren, S. K. (1898). About the theory of so-called adsorption of soluble substances. *Sven. Vetenskapsakad. Handingarl, 24,* 1-39.

Langmuir, I. (1918). The adsorption of gases on plane surfaces of glass, mica and platinum. *Journal of the American Chemical Society, 40*(9), 1361-1403. https://doi.org/10.1021/ja02242a004

Lellis, B., Fávaro-Polonio, C. Z., Pamphile, J. A., & Polonio, J. C. (2019). Effects of textile dyes on health and the environment and bioremediation potential of living organisms. *Biotechnology Research and Innovation, 3*(2), 275-290.

Li, Q., Li, Y., Li, Y., Chen, Y., Wu, Q., & Wang, S. (2021). Efficient removal of methyl orange by nanocomposite aerogel of polyethyleneimine and B -CYCLODEXTRIN grafted cellulose nanocrystals. *Journal of Applied Polymer Science, 138*(48), 51481. https://doi.org/10.1002/app.51481

Li, W., Zhang, L., Hu, D., Yang, R., Zhang, J., Guan, Y., Lv, F., & Gao, H. (2021). A mesoporous nanocellulose/sodium alginate/carboxymethyl-chitosan gel beads for efficient adsorption of Cu2+ and Pb2+. *International Journal of Biological Macromolecules, 187,* 922-930. https://doi.org/10.1016/j.ijbiomac.2021.07.181

Li, Y., Zhang, L., Song, Z., Li, F., & Xie, D. (2022). Intelligent temperature-pH dual responsive nanocellulose hydrogels and the application of drug release towards 5-fluorouracil. *International Journal of Biological Macromolecules, 223,* 11-16. https://doi.org/10.1016/j.ijbiomac.2022.10.188

Lim, M. B., Hu, M., Manandhar, S., Sakshaug, A., Strong, A., Riley, L., & Pauzauskie, P. J. (2015). Ultrafast sol-gel synthesis of graphene aerogel materials. *Carbon, 95,* 616-624. https://doi.org/10.1016/j.carbon.2015.08.037

Lin, K., Sun, W., Feng, L., Wang, H., Feng, T., Zhang, J., Cao, M., Zhao, S., Yuan, Y., & Wang, N. (2022). Kelp inspired bio-hydrogel with high antibiofouling activity and super-toughness for ultrafast uranium extraction from seawater. *Chemical Engineering Journal, 430,* 133121.

Long, L.-Y., Weng, Y.-X., & Wang, Y.-Z. (2018). Cellulose Aerogels: Synthesis, Applications, and Prospects. *Polymers, 10*(6), 623. https://doi.org/10.3390/polym10060623

Lu, F., & Astruc, D. (2020). Nanocatalysts and other nanomaterials for water remediation from organic pollutants. *Coordination Chemistry Reviews, 408,* 213180. https://doi.org/10.1016/j.ccr.2020.213180

Mahfoudhi, N., & Boufi, S. (2017). Nanocellulose as a novel nanostructured adsorbent for environmental remediation: A review. *Cellulose*, *24*(3), 1171-1197. https://doi.org/10.1007/s10570-017-1194-0

Malik, R., Warkar, S. G., & Saxena, R. (2023). Carboxy-methyl tamarind kernel gum based bio-hydrogel for sustainable agronomy. *Materials Today Communications*, *35*, 105473.

Mishnaevsky, L., Mikkelsen, L. P., Gaduan, A. N., Lee, K.-Y., & Madsen, B. (2019). Nanocellulose reinforced polymer composites: Computational analysis of structure-mechanical properties relationships. *Composite Structures*, *224*, 111024. https://doi.org/10.1016/j.compstruct.2019.111024

Mohammadinejad, R., Maleki, H., Larrañeta, E., Fajardo, A. R., Nik, A. B., Shavandi, A., Sheikhi, A., Ghorbanpour, M., Farokhi, M., Govindh, P., Cabane, E., Azizi, S., Aref, A. R., Mozafari, M., Mehrali, M., Thomas, S., Mano, J. F., Mishra, Y. K., & Thakur, V. K. (2019). Status and future scope of plant-based green hydrogels in biomedical engineering. *Applied Materials Today*, *16*, 213-246. https://doi.org/10.1016/j.apmt.2019.04.010

Mohite, P. B., & Adhav, S. S. (2017). A hydrogels: Methods of preparation and applications. *Int. J. Adv. Pharm*, *6*(3), 79-85.

Mullet, M., Fievet, P., Szymczyk, A., Foissy, A., Reggiani, J.-C., & Pagetti, J. (1999). A simple and accurate determination of the point of zero charge of ceramic membranes. *Desalination*, *121*(1), 41-48. https://doi.org/10.1016/S0011-9164(99)00006-5

Nasution, H., Harahap, H., Dalimunthe, N. F., Ginting, M. H. S., Jaafar, M., Tan, O. O., Aruan, H. K., & Herfananda, A. L. (2022). Hydrogel and effects of crosslinking agent on cellulose-based hydrogels: A review. *Gels*, *8*(9), 568.

Nguyen, V. T., Ha, L. Q., Nguyen, T. D. L., Ly, P. H., Nguyen, D. M., & Hoang, D. (2022). Nanocellulose and Graphene Oxide Aerogels for Adsorption and Removal Methylene Blue from an Aqueous Environment. *ACS Omega*, *7*(1), 1003-1013. https://doi.org/10.1021/acsomega.1c05586

Paul, J., & Ahankari, S. S. (2023). Nanocellulose-based aerogels for water purification: A review. *Carbohydrate Polymers*, 120677.

Piaskowski, K., Świderska-Dąbrowska, R., & Zarzycki, P. K. (2018). Dye removal from water and wastewater using various physical, chemical, and biological processes. *Journal of AOAC International*, *101*(5), 1371-1384.

Piccin, J. S., Dotto, G. L., & Pinto, L. A. A. (2011). Adsorption isotherms and thermochemical data of FD&C Red n° 40 binding by Chitosan. *Brazilian Journal of Chemical Engineering*, *28*(2), 295-304. https://doi.org/10.1590/S0104-66322011000200014

Pooresmaeil, M., & Namazi, H. (2020). Application of polysaccharide-based hydrogels for water treatments. In *Hydrogels based on natural polymers* (pp. 411-455). Elsevier.

Poornachandhra, C., Jayabalakrishnan, R. M., Prasanthrajan, M., Balasubramanian, G., Lakshmanan, A., Selvakumar, S., & John, J. E. (2023). Cellulose-based hydrogel for adsorptive removal of cationic dyes from aqueous solution: Isotherms and kinetics. *RSC Advances*, *13*(7), 4757-4774. https://doi.org/10.1039/D2RA08283G

Radakisnin, R., Abdul Majid, M. S., Jamir, M. R. M., Jawaid, M., Sultan, M. T. H., & Mat Tahir, M. F. (2020). Structural, morphological and thermal properties of cellulose nanofibers from Napier fiber (Pennisetum purpureum). *Materials*, *13*(18), 4125.

Raj, S., Singh, H., Trivedi, R., & Soni, V. (2020). Biogenic synthesis of AgNPs employing Terminalia arjuna leaf extract and its efficacy towards catalytic degradation of organic dyes. *Scientific Reports*, *10*(1), 9616. https://doi.org/10.1038/s41598-020-66851-8

Rana, A. K. (2022). Green Approaches in the Valorization of Plant Wastes: Recent Insights and Future Directions. *Current Opinion in Green and Sustainable Chemistry*, 100696.

Rana, A. K., Frollini, E., & Thakur, V. K. (2021). Cellulose nanocrystals: Pretreatments, preparation strategies, and surface functionalization. *International Journal of Biological Macromolecules*, *182*, 1554-1581.

Rana, A. K., Guleria, S., Gupta, V. K., & Thakur, V. K. (2022). Cellulosic pine needles-based biorefinery for a circular bioeconomy. *Bioresource Technology*, 128255.

Rana, A. K., Gupta, V. K., Saini, A. K., Voicu, S. I., Abdellattifaand, M. H., & Thakur, V. K. (2021). Water desalination using nanocelluloses/cellulose derivatives based membranes for sustainable future. *Desalination*, *520*, 115359.

Rana, A. K., Mishra, Y. K., Gupta, V. K., & Thakur, V. K. (2021). Sustainable materials in the

removal of pesticides from contaminated water: Perspective on macro to nanoscale cellulose. *Science of The Total Environment, 797,* 149129.

Rana, A. K., Mostafavi, E., Alsanie, W. F., Siwal, S. S., & Thakur, V. K. (2023). Cellulose-based materials for air purification: A review. *Industrial Crops and Products, 194*, 116331. https://doi.org/10.1016/j.indcrop.2023.116331

Rana, A. K., Scarpa, F., & Thakur, V. K. (2022). Cellulose/polyaniline hybrid nanocomposites: Design, fabrication, and emerging multidimensional applications. *Industrial Crops and Products, 187,* 115356.

Rao, K. M., Kumar, A., & Han, S. S. (2017). Poly(acrylamidoglycolic acid) nanocomposite hydrogels reinforced with cellulose nanocrystals for pH-sensitive controlled release of diclofenac sodium. *Polymer Testing, 64,* 175-182. https://doi.org/10.1016/j.polymertesting.2017.10.006

Roa, K., Tapiero, Y., Thotiyl, M. O., & Sánchez, J. (2021). Hydrogels Based on Poly([2-(acryloxy)ethyl] Trimethylammonium Chloride) and Nanocellulose Applied to Remove Methyl Orange Dye from Water. *Polymers, 13*(14), 2265. https://doi.org/10.3390/polym13142265

Ruan, C., Ma, Y., Shi, G., He, C., Du, C., Jin, X., Liu, X., He, S., & Huang, Y. (2022). Self-assembly cellulose nanocrystals/SiO_2 composite aerogel under freeze-drying: Adsorption towards dye contaminant. *Applied Surface Science, 592,* 153280. https://doi.org/10.1016/j.apsusc.2022.153280

Safavi-Mirmahalleh, S.-A., Salami-Kalajahi, M., & Roghani-Mamaqani, H. (2020). Adsorption kinetics of methyl orange from water by pH-sensitive poly (2-(dimethylamino) ethyl methacrylate)/nanocrystalline cellulose hydrogels. *Environmental Science and Pollution Research, 27,* 28091-28103.

Shaheed, N., Javanshir, S., Esmkhani, M., Dekamin, M. G., & Naimi-Jamal, M. R. (2021). Synthesis of nanocellulose aerogels and Cu-BTC/nanocellulose aerogel composites for adsorption of organic dyes and heavy metal ions. *Scientific Reports, 11*(1), 18553. https://doi.org/10.1038/s41598-021-97861-9

Shak, K. P. Y., Pang, Y. L., & Mah, S. K. (2018). Nanocellulose: Recent advances and its prospects in environmental remediation. *Beilstein Journal of Nanotechnology, 9*(1), 2479-2498.

Shandong Agricultural University, Wei, J., Gui, S.-H., Shandong Agricultural University, Wu, J.-H., Shandong Agricultural University, Xu, D.-D., Shandong Agricultural University, Sun, Y., Shandong Agricultural University, Dong, X.-Y., Shandong Agricultural University, Dai, Y.-Y., Shandong Agricultural University, Li, Y.-F., & Shandong Agricultural University. (2019). Nanocellulose-Graphene Oxide Hybrid Aerogel to Water Purification. *Applied Environmental Biotechnology, 4*(1), 11-17. https://doi.org/10.26789/AEB.2019.01.003

Sharma, A., Mandal, T., & Goswami, S. (2021). Dispersibility and stability studies of cellulose nanofibers: Implications for nanocomposite preparation. *Journal of Polymers and the Environment, 29,* 1516-1525.

Sharma, P., Kherb, J., Prakash, J., & Kaushal, R. (2023). A novel and facile green synthesis of SiO_2 nanoparticles for removal of toxic water pollutants. *Applied Nanoscience, 13*(1), 735-747. https://doi.org/10.1007/s13204-021-01898-1

Sharma, P., Prakash, J., & Kaushal, R. (2022). An insight into the green synthesis of SiO_2 nanostructures as a novel adsorbent for removal of toxic water pollutants. *Environmental Research, 212,* 113328. https://doi.org/10.1016/j.envres.2022.113328

Sharma, P., Prakash, J., Palai, T., & Kaushal, R. (2022). Surface functionalization of bamboo leave mediated synthesized SiO_2 nanoparticles: Study of adsorption mechanism, isotherms and enhanced adsorption capacity for removal of Cr (VI) from aqueous solution. *Environmental Research, 214,* 113761. https://doi.org/10.1016/j.envres.2022.113761

Sharma, V., Shahnaz, T., Subbiah, S., & Narayanasamy, S. (2020). New insights into the remediation of water pollutants using nanobentonite incorporated nanocellulose chitosan based aerogel. *Journal of Polymers and the Environment, 28,* 2008-2019.

Singha, A. S., & Rana, A. K. (2012). Preparation and characterization of graft copolymerized Cannabis indica L. fiber-reinforced unsaturated polyester matrix-based biocomposites. *Journal of Reinforced Plastics and Composites, 31*(22), 1538-1553.

Sinha, V., & Chakma, S. (2019). Advances in the preparation of hydrogel for wastewater treatment: A concise review. *Journal of Environmental Chemical Engineering, 7*(5), 103295. https://doi.org/10.1016/j.jece.2019.103295

Sips, R. (1948). On the Structure of a Catalyst Surface. *The Journal of Chemical Physics, 16*(5), 490-495. https://doi.org/10.1063/1.1746922

Solayman, H. M., Hossen, M. A., Abd Aziz, A., Yahya, N. Y., Hon, L. K., Ching, S. L., Monir, M. U., & Zoh, K.-D. (2023). Performance evaluation of dye wastewater treatment technologies: A review. *Journal of Environmental Chemical Engineering*, 109610.

Sultana, H., & Usman, M. (2023). Surfactant-assisted flocculation for the efficient removal of aqueous dyestuff: A sustainable approach. *Journal of Molecular Liquids, 370*, 120988.

Taher, T., Munandar, A., Mawaddah, N., Wisnubroto, M. S., Siregar, P. M. S. B. N., Palapa, N. R., Lesbani, A., & Wibowo, Y. G. (2023). Synthesis and characterization of montmorillonite-Mixed metal oxide composite and its adsorption performance for anionic and cationic dyes removal. *Inorganic Chemistry Communications, 147*, 110231.

Tang, J., Song, Y., Zhao, F., Spinney, S., Da Silva Bernardes, J., & Tam, K. C. (2019). Compressible cellulose nanofibril (CNF) based aerogels produced via a bio-inspired strategy for heavy metal ion and dye removal. *Carbohydrate Polymers, 208*, 404-412. https://doi.org/10.1016/j.carbpol.2018.12.079

Tavakolian, M., Wiebe, H., Sadeghi, M. A., & Van De Ven, T. G. M. (2020). Dye Removal Using Hairy Nanocellulose: Experimental and Theoretical Investigations. *ACS Applied Materials & Interfaces, 12*(4), 5040-5049. https://doi.org/10.1021/acsami.9b18679

Temkin, M. I. (1940). Kinetics of ammonia synthesis on promoted iron catalysts. *Acta Physiochim. URSS, 12*, 327-356.

Thakur, M. K., Rana, A. K., & Thakur, V. K. (2014). Lignocellulosic polymer composites: A brief overview. *Lignocellulosic Polymer Composites: Processing, Characterization, and Properties. Vol. 9781118773574, Wiley Blackwell*, 1-15.

Thakur, S., Chaudhary, J., Thakur, A., Gunduz, O., Alsanie, W. F., Makatsoris, C., & Thakur, V. K. (2022). Highly efficient poly(acrylic acid-co-aniline) grafted itaconic acid hydrogel: Application in water retention and adsorption of rhodamine B dye for a sustainable environment. *Chemosphere, 303*, 134917. https://doi.org/10.1016/j.chemosphere.2022.134917

Thakur, S., Verma, A., Kumar, V., Jin Yang, X., Krishnamurthy, S., Coulon, F., & Thakur, V. K. (2022). Cellulosic biomass-based sustainable hydrogels for wastewater remediation: Chemistry and prospective. *Fuel, 309*, 122114. https://doi.org/10.1016/j.fuel.2021.122114

Tshikovhi, A., Mishra, S. B., & Mishra, A. K. (2020). Nanocellulose-based composites for the removal of contaminants from wastewater. *International Journal of Biological Macromolecules, 152*, 616-632.

Tzabar, N., & Ter Brake, H. J. M. (2016). Adsorption isotherms and Sips models of nitrogen, methane, ethane, and propane on commercial activated carbons and polyvinylidene chloride. *Adsorption, 22*(7), 901-914. https://doi.org/10.1007/s10450-016-9794-9

Vakili, M. R., Mohammed-Saeid, W., Aljasser, A., Hopwood-Raja, J., Ahvazi, B., Hrynets, Y., Betti, M., & Lavasanifar, A. (2021). Development of mucoadhesive hydrogels based on polyacrylic acid grafted cellulose nanocrystals for local cisplatin delivery. *Carbohydrate Polymers, 255*, 117332. https://doi.org/10.1016/j.carbpol.2020.117332

Vasconcelos, N. F., Feitosa, J. P. A., da Gama, F. M. P., Morais, J. P. S., Andrade, F. K., de Souza, M. de S. M., & de Freitas Rosa, M. (2017). Bacterial cellulose nanocrystals produced under different hydrolysis conditions: Properties and morphological features. *Carbohydrate Polymers, 155*, 425-431.

Wang, H., Wang, Y., & Dionysiou, D. D. (2023). Advanced oxidation processes for removal of emerging contaminants in water. In *Water* (Vol. 15, Issue 3, p. 398). MDPI.

Wang, M., Song, Y., Bisoyi, H. K., Yang, J., Liu, L., Yang, H., & Li, Q. (2021). A Liquid Crystal Elastomer-Based Unprecedented Two-Way Shape-Memory Aerogel. *Advanced Science, 8*(22), 2102674. https://doi.org/10.1002/advs.202102674

Wang, Z., Song, L., Wang, Y., Zhang, X.-F., Hao, D., Feng, Y., & Yao, J. (2019). Lightweight UiO-66/cellulose aerogels constructed through self-crosslinking strategy for adsorption applications. *Chemical Engineering Journal, 371*, 138-144. https://doi.org/10.1016/j.cej.2019.04.022

Wang, Z., Song, L., Wang, Y., Zhang, X.-F., & Yao, J. (2021). Construction of a hybrid graphene oxide/nanofibrillated cellulose aerogel used for the efficient removal of methylene blue and tetracycline. *Journal of Physics and Chemistry of*

Solids, *150*, 109839. https://doi.org/10.1016/j.jpcs.2020.109839

Water Futures and Solutions (WFaS). (n.d.). IIASA - International Institute for Applied Systems Analysis. Retrieved August 15, 2023, from https://iiasa.ac.at/projects/wfas

Water scarcity | UNICEF. (n.d.). Retrieved August 15, 2023, from https://www.unicef.org/wash/water-scarcity

Weber, W. J., & Morris, J. C. (1963). Kinetics of Adsorption on Carbon from Solution. *Journal of the Sanitary Engineering Division*, *89*(2), 31-59. https://doi.org/10.1061/JSEDAI.0000430

Wu, P., Zhang, B., Yu, Z., Zou, H., & Liu, P. (2019). Anisotropic polyimide aerogels fabricated by directional freezing. *Journal of Applied Polymer Science*, *136*(11), 47179. https://doi.org/10.1002/app.47179

Wu, Q., Li, X., Fu, S., Li, Q., & Wang, S. (2017). Estimation of aspect ratio of cellulose nanocrystals by viscosity measurement: Influence of surface charge density and NaCl concentration. *Cellulose*, *24*(8), 3255-3264. https://doi.org/10.1007/s10570-017-1341-7

Xia, H., Li, C., Yang, G., Shi, Z., Jin, C., He, W., Xu, J., & Li, G. (2022). A review of microwave-assisted advanced oxidation processes for wastewater treatment. *Chemosphere*, *287*, 131981.

Xue, J., Zhu, E., Zhu, H., Liu, D., Cai, H., Xiong, C., Yang, Q., & Shi, Z. (2023). Dye adsorption performance of nanocellulose beads with different carboxyl group content. *Cellulose*, *30*(3), 1623-1636. https://doi.org/10.1007/s10570-022-04964-1

Yap, J. X., Leo, C. P., Derek, C. J. C., Yasin, N. H. M., & Sajab, M. S. (2023). Chlorella vulgaris nanocellulose in hydrogel beads for dye removal. *Separation and Purification Technology*, 124613.

Yaseen, D. A., & Scholz, M. (2019). Textile dye wastewater characteristics and constituents of synthetic effluents: A critical review. *International Journal of Environmental Science and Technology*, *16*, 1193-1226.

Yin, Y., Lucia, L. A., Pal, L., Jiang, X., & Hubbe, M. A. (2020). Lipase-catalyzed laurate esterification of cellulose nanocrystals and their use as reinforcement in PLA composites. *Cellulose*, *27*, 6263-6273.

Zain, Z. M., Abdulhameed, A. S., Jawad, A. H., ALOthman, Z. A., & Yaseen, Z. M. (2023). A pH-sensitive surface of chitosan/sepiolite clay/algae biocomposite for the removal of malachite green and remazol brilliant blue R dyes: Optimization and adsorption mechanism study. *Journal of Polymers and the Environment*, *31*(2), 501-518.

Zainal, S. H., Mohd, N. H., Suhaili, N., Anuar, F. H., Lazim, A. M., & Othaman, R. (2021). Preparation of cellulose-based hydrogel: A review. *Journal of Materials Research and Technology*, *10*, 935-952.

Zhang, T., Xiao, S., Fan, K., He, H., & Qin, Z. (2022). Preparation and adsorption properties of green cellulose-based composite aerogel with selective adsorption of methylene blue. *Polymer*, *258*, 125320. https://doi.org/10.1016/j.polymer.2022.125320

Zhang, W., Wang, X., Zhang, Y., Van Bochove, B., Mäkilä, E., Seppälä, J., Xu, W., Willför, S., & Xu, C. (2020). Robust shape-retaining nanocellulose-based aerogels decorated with silver nanoparticles for fast continuous catalytic discoloration of organic dyes. *Separation and Purification Technology*, *242*, 116523. https://doi.org/10.1016/j.seppur.2020.116523

Zhang, W., Zhang, M., Yao, J., & Long, J. (2023). Industrial indigo dyeing wastewater purification: Effective COD removal with peroxi-AC electrocoagulation system. *Arabian Journal of Chemistry*, *16*(4), 104607.

Zhang, X., Elsayed, I., Navarathna, C., Schueneman, G. T., & Hassan, E. B. (2019). Biohybrid Hydrogel and Aerogel from Self-Assembled Nanocellulose and Nanochitin as a High-Efficiency Adsorbent for Water Purification. *ACS Applied Materials & Interfaces*, *11*(50), 46714-46725. https://doi.org/10.1021/acsami.9b15139

Zhang, X., Li, F., Zhao, X., Cao, J., Liu, S., Zhang, Y., Yuan, Z., Huang, X., De Hoop, C. F., Peng, X., & Huang, X. (2023). Bamboo Nanocellulose/Montmorillonite Nanosheets/Polyethyleneimine Gel Adsorbent for Methylene Blue and Cu(II) Removal from Aqueous Solutions. *Gels*, *9*(1), 40. https://doi.org/10.3390/gels9010040

Zhang, Z., Abidi, N., Lucia, L., Chabi, S., Denny, C. T., Parajuli, P., & Rumi, S. (2022). Cellulose/nanocellulose superabsorbent hydrogels as a sustainable platform for materials applications: A mini-review. *Carbohydrate Polymers*, 120140.

Zhang, Z., Hu, J., Tian, X., Guo, F., Wang, C., Zhang, J., & Jiang, M. (2022). Facile in-situ growth of metal-organic framework layer on carboxylated nanocellulose/chitosan aerogel

spheres and their high-efficient adsorption and catalytic performance. *Applied Surface Science, 599,* 153974. https://doi.org/10.1016/j.apsusc.2022.153974

Zhao, H., Zhang, Y., Liu, Y., Zheng, P., Gao, T., Cao, Y., Liu, X., Yin, J., & Pei, R. (2021). In Situ Forming Cellulose Nanofibril-Reinforced Hyaluronic Acid Hydrogel for Cartilage Regeneration. *Biomacromolecules, 22*(12), 5097-5107. https://doi.org/10.1021/acs.biomac.1c01063

Zheng, A. L. T., Sabidi, S., Ohno, T., Maeda, T., & Andou, Y. (2022). Cu_2O/TiO_2 decorated on cellulose nanofiber/reduced graphene hydrogel for enhanced photocatalytic activity and its antibacterial applications. *Chemosphere, 286,* 131731. https://doi.org/10.1016/j.chemosphere.2021.131731

Zubik, K., Singhsa, P., Wang, Y., Manuspiya, H., & Narain, R. (2017). Thermo-Responsive Poly(N-Isopropylacrylamide)-Cellulose Nanocrystals Hybrid Hydrogels for Wound Dressing. *Polymers, 9*(12), 119. https://doi.org/10.3390/polym9040119

Zuo, L., Zhang, Y., Zhang, L., Miao, Y.-E., Fan, W., & Liu, T. (2015). Polymer/Carbon-Based Hybrid Aerogels: Preparation, Properties and Applications. *Materials, 8*(10), 6806-6848. https://doi.org/10.3390/ma8105343